Copyright Warning & Restrictions

The copyright law of the United States (Title 17, United States Code) governs the making of photocopies or other reproductions of copyrighted material.

Under certain conditions specified in the law, libraries and archives are authorized to furnish a photocopy or other reproduction. One of these specified conditions is that the photocopy or reproduction is not to be "used for any purpose other than private study, scholarship, or research." If a, user makes a request for, or later uses, a photocopy or reproduction for purposes in excess of "fair use" that user may be liable for copyright infringement,

This institution reserves the right to refuse to accept a copying order if, in its judgment, fulfillment of the order would involve violation of copyright law.

Please Note: The author retains the copyright while the New Jersey Institute of Technology reserves the right to distribute this thesis or dissertation

Printing note: If you do not wish to print this page, then select "Pages from: first page # to: last page #" on the print dialog screen

NJIT New Jersey's Science & Technology University

The Van Houten library has removed some of the personal information and all signatures from the approval page and biographical sketches of theses and dissertations in order to protect the identity of NJIT graduates and faculty.

NON-LINEAR FINITE ELEMENT ANALYSIS

OF

REINFORCED CONCRETE MEMBERS

by

CHELLATHURAI JEYAMOHAN

Thesis submitted to the faculty of the Graduate School of the New Jersey Institute of Technology in partial fulfillment of the requirements for the degree of Master of Science in Civil Engineering.

1987

APPROVAL SHEET

Title of Thesis : Non-Linear Finite Element Analysis of Reinforced Comcrete Members.

Name of Candidate : Chellathurai Jeyamohan
Master of Science in Civil Engineering, 1987.

Thesis and Abstract Approved :

.....
C.T.THOMAS HSU
Professor
of Civil Engineering,
Department of Civil and
Environmental Engineering.

.....
DATE

.....
DATE

.....
DATE

VITAE

Name : Chellathurai Jeyamohan

Address :

Degree and Date to be conferred : M.S. Civil Engineering, 1987.

Date of birth :

Place of birth :

Collegiate Institutions attended	Dates	Degree
University of Sri Lanka	1974-1978	B.S.C.E
New Jersey Institute of Technology	1984-1987	M.S.C.E

Major : Structural Engineering

ABSTRACT

Title of Thesis : Non-Linear Finite Element Analysis of Reinforced Concrete Members.

by : Chellathurai Jeyamohan

Thesis Directed by : Professor C.T.Thomas Hsu

A finite element analysis of reinforced concrete members is used to study the initiation and propagation of cracks and the behavior at the interface of concrete and steel. The increase of concrete strength due to the biaxial compression and the shear capacity of the cracked elements are also considered in the analysis.

The results of the present analysis are compared with some available experimental data in beam tests. It has been found that the present analysis is capable of calculating the stress (or moment) and strain (or deformation) from zero load upto the ultimate load.

ACKNOWLEDGEMENTS

The thesis , presented here , commenced under the guidance of Professor C.T.Thomas Hsu. I wish to express my sincere thanks to Dr.Thomas Hsu whose continuous assistance and constant encouragement in the execution of the program.

I wish to thank my wife for her support in helping me to complete this thesis.

TABLE OF CONTENTS

CHAPTER 1 Introduction and Literature Review

1.1 General

1.2 Historical review of finite element analysis of reinforced concrete structures.

1.3 Literature Review

1.3.1 Elasticity based models

1.3.2 Plasticity based model

1.3.3 Cracking models

1.3.4 Steel concrete interface behaviour

1.3.5 Post cracking shear behaviour

1.3.6 Tension stiffening effect

CHAPTER 2 Finite element model for planar structures.

2.1 Introduction

2.2 Concrete and steel representation

2.2.1 Linear displacement quadrilateral element

2.2.1.1 Displacement functions

2.3 Strain-displacement relationship

2.4 stress-strain relationship

2.5 Formulation of element stiffness matrix

CHAPTER 3 Finite Element Analysis in Concrete Structures

3.1 Introduction to displacement formulation

3.2 Finite element mesh

3.3 Properties of cross-section

3.4 Constitutive relation of concrete

3.4.1 Behaviour of concrete under uniaxial tension

3.4.2 Behaviour of concrete under uniaxial compression

3.4.3 Biaxial behaviour of concrete

3.4.4 Orthotropic stress-strain relations

3.4.5 Properties of steel

3.4.6 Failure criterion of concrete

3.5 Steel concrete interface behaviour

3.5.1 Forces at interface

3.5.2 Stiffness of linkage element

3.5.3 Bond stress-slip relationships

3.5.4 Bond failure criteria

3.5.5 Dowel action

3.6 Stirrups

3.7 Cracking

CHAPTER 4 Analysis of results

4.1 Introduction

4.2 Singly reinforced simply supported beam

4.2.1 Description

4.2.2 Interpretation of results

4.2.2.1 Elastic range of loading

4.2.2.2 Crack initiation and propagation

4.3 Doubly Reinforced Simply Supported Beam

4.3.1 Description

4.3.2 Interpretation of Results

4.3.2.1 Elastic range of loading

4.3.2.2 Crack initiation and propagation

CHAPTER 5 Summary and Conclusions

5.1 Summary and conclusions

5.2 Suggestions for future research

References

APPENDIX Input Information

CHAPTER 1

INTRODUCTION AND LITERATURE REVIEW

1.1 GENERAL

The analysis of structural members and structural systems are commonly done by moment distribution, slope deflection and matrix method of structural analysis. When the shape of the members become complex , all the above methods require either simplification of member characteristics or the analysis becomes very tedious though not impossible.

The finite element analysis of steel members and steel structures are not that complicated compared to the reinforced concrete members or systems. The following factors make the finite element analysis of reinforced concrete members very difficult.

(1) Concrete is a non-homogeneous material. Its behaviour is very hard to be put in a simple mathematical formula. Material properties are found to vary in directions, from point to point, with different type of loadings such as monotonic increasing and cyclic loadings and in the different state of stress combination that might have been caused by varying loading system.

(2) The behavior of steel concrete interface is not well understood and is a complex three dimensional phenomenon.

(3) The behavior of concrete and the transfer of forces across a cracked section after the cracks are formed , are not understood clearly.

Despite the lack of informations on material behavior and difficulties encountered in the finite element analysis of reinforced concrete members , many researchers and analysts successfully formulated models to represent or simulate each action and analysed the members or systems quite effectively.

1.2 HISTORICAL REVIEW OF FINITE ELEMENT ANALYSIS OF RC STRUCTURES

The following paragraphs are some of the works carried out by researchers , and show how the analysis got reformed and refined over the period of time.

Scordelis and Ngo (3) analysed simple beams. The triangular elements represented the concrete and steel. Bond stress - slip phenomenon was successfully incorporated with the use of linkage element concept. Material behaviors of steel and concrete were assumed to be fully elastic. Predicted crack patterns were considered in the analysis.

Nilson(4) performed a non-linear analysis. The concrete stress-strain relationship suggested by Saenz (5) was used to represent the concrete behavior . His formulationof bond stress-slip expressions were differentiated to obtain

the stiffness parameters of the linkage elements to portray the concrete steel interface behavior . An incremental loading technique was employed and every time an element cracked , the topology was redefined and the computer run commenced again until the required load level was achieved.

The model developed by Franklin(7) accounted automatically for cracking and redistribution of stresses not balanced internally , thereby enabling to execute the analysis in one computer run without being redefining the topology every time an element cracked. He analysed the effects of reinforced concrete frames with and without reinforced concrete shear walls. Special types of frame elements and quadrilateral elements represented members and joints.

Cervenka and Gerstle(8) analysed shear panels. Both steel and concrete were assumed to be elastic-perfectly plastic. Composite material constitutive relationship was used to develop the stress-strain stiffness matrix.

Yuzugullu and Schnobrich(9) studied the inelastic behavior of frame-shear wall system. Shear wall and frame were represented by quadrilateral and flexural elements respectively. The interface action between shear wall and framewas modelled by linkage elements containing two orthogonal springs. Composite material constitutive relationship was used. After cracking , cracked element's shear modulus

was reduced to a fraction of its original value to account for the load transferring behavior across the crack.

Cedolin and Del Poli(10) made a non linear analysis on shallow beams. Concrete and steel were represented by triangular elements and the stirrups by one dimensional bar elements. Concrete was assumed to have two different modulii E1 ,E2 in orthogonal directions. Linkage elements represented the effects at steel concrete interface.

Darwin and Pecknold(13) did a non-linear finite element analysis on a planar concrete members subjected to cyclic loadings.

Agrawal(14) performed a non linear analysis of a reinforced concrete deep beam subjected to cyclic loading. Both steel and concrete were assumed to behave like an elastic-perfectly plastic material. Each node had three degrees of freedom. A composite material constitutive relationship was used.

Al-Mahaidi(15) also performed a non linear analysisof reinforced concrete deep beams. Quadrilateral and base elements represented concrete and steel. Concrete was assumed to follow an orthotropic material having two different elastic modulii in orthogonal directions. Steel reinforcement followed an elastic perfectly plastic material behavior. Bond stress - slip relation provided the stiffnesses of linkage

element springs which modelled the interface behavior. Both discrete smeared cracking models analysed the deep beams.

Spokowski(17) used non linear finite element analysis on reinforced concrete beams and joints. The analysis predicted the load - deflection curves , moment - rotation relationships and crack patterns. Discrete cracking model was used after the element had cracked , redistribution of stresses were made to account for unbalanced forces.

Houde(18) derived an empirical expression for the transfer of shear across a crack and incorporated his findings in the finite element program. The program incorporated his expression to analyse pull-out specimens and beams.

Khouzam(19) used Houde's expression for the shear transfer across a crack and carried out a non-linear analysis of axially loaded tensile members and reinforced concrete beams with unreinforced webs.

The historical development suggests that the finite element analysis has been a valuable tool to many researchers in analysing reinforced concrete structural members and systems. The accuracy of the method would increase if the following behaviors can be understood thoroughly and expressed properly in the formulation of the finite element program.

(1) Material behavior of concrete under different stress

states

(2) Steel behavior under different stress states

(3) Steel concrete interface action

(4) Force transfer mechanism across a cracked concrete section , specifically aggregate interlock and dowel action.

1.3 REVIEW OF LITERATURE

In the following paragraphs a historical review of material behaviors , steel concrete interface action and post cracking behavior is presented.

1.3.1 CONCRETE STRESS-STRAIN BEHAVIOR

The stress-strain behavior of concrete has a significant effect on the accuracy of the predictions of any finite element analysis of reinforced or plain concrete members. Researchers used either elasticity based models or plasticity based models to represent the behavior of concrete.

1.3.1.1 ELASTICITY BASED MODELS

Two different approaches are used here to model the stress-strain behavior.

(1) Total stress strain model

(2) Incremental stress strain model

In the total stress strain model , the total stress of a stress state is assumed to be uniquely determined as a function of the present total strain. The assumption itself imposes a limitation on these type of models because of the path dependent charecteristics of concrete. Therefore , the application of these models is restricted and used only to monotonically increasing loads.

In the incremental elasticity model , the behavior of the material is assumed to depend on the present state of stress and strain as well as on the path followed to reach the existing state. Therefore , we may conclude that incremental elasticity model provides more realistic behavior of stress strain relationship under cyclic loading conditions. These models can be further refined to include the orthotropic properties with the principal stress directions coinciding with the directions of orthotropy.

Elasticity based models are popularly used in the non linear finite element analysis because of their simplicity. They provide a reasonable representation of the overall behavior of concrete but some of them poorly represents the behavior near the ultimate state. This drawback has not caused any major problem because only a very small portion of concrete reaches the ultimate stress state and the rest of the concrete can be represented quite well with this model.

1.3.2 PLASTICITY BASED MODEL

Two approaches are available to characterise the stress-strain behavior.

(a) Elastic-strain hardening plastic

(b) Plastic fracturing models

In the elastic strain hardening plastic models , a discontinuity surface is introduced , which is the limiting surface for elastic behavior , and located at a distance from the fracturing surface. When a material is stressed beyond the initial discontinuity surface , a new discontinuity surface called the loading surface is created. Loading and unloading within any two subsequent loading surfaces result in elastic behavior. Irrecoverable plastic strains will occur only if the upper loading surface is crossed. The final collapse of the concrete will occur only when the loading surface reaches the fracture surface. A detail explanation and formulation of constitutive matrix for an elastic-strain hardening plastic and plastic fracturing models appear in Ref:(30). The following paragraphs briefly gives the works of researchers used in the modelling of concrete stress-strain behavior

Ngo and Scordelis(3) used linear isotropic material models in their analysis.

Kupfer and Gerstle(23) presented closed form expressions for shear and bulk modulus of concrete and used total stress-strain behavior models in their work. The suggested closed form expressions were obtained to match the experimental data made available from different sets of concrete specimen under different state of biaxial stress system.

Romstad, Taylor and Herrmann(24) developed a biaxial isotropic stress-strain model. Number of damaged regions were created and the material properties were altered to match the degradation of concrete caused by increased stresses. Modulus of elasticity and Poisson's ratio remained constant within each damaged region.

Gerstle(25) developed a biaxial incrementally isotropic stress-strain model. Bulk and shear modulii are assumed to be a linear function of the octahedral normal and shear stresses. Constitutive matrix was expressed in terms of bulk and shear modulus.

Darwin and Pecknold(13) proposed a biaxial incrementally isotropic stress-strain behavior. A new equivalent uniaxial strain concept was introduced. The effect of a biaxial stress system on a concrete is represented by equivalent stress-strain curves for each of the principal axes direction.
A biaxial incrementally orthotropic stress-strain behavior was forwarded by Liu , Nelson and Slate(12,26).

Bazant and Tsubaki(27) suggested a triaxial total stress-strain behavior model. The constitutive matrix comprised of bulk and shear modulus which were expressed as the functions of first and second invariants of the total stress and strain tensors.

Elwi and Murray (28) developed a triaxial incrementally isotropic stress-strain model.The equivalent uniaxial strain concept was employed in deriving the constitutive matrix.

1.3.3 CRACKING MODELS

The magnitude of tensile stress , at which concrete fails in tension is not a unique value thereby causing difficulties in the modeling of cracking of concrete. Despite the uncertainities and complex nature of cracking , two different cracking models were advanced by researchers to represent the cracking phenomenon in concrete.

a. Discrete Cracking Model:

Adjoining elements are disconnected at the nodes along their boundaries when an element cracks and causes displacement discontinuities across the crack. The introduction of additional nodal points required to redefine the topology after a crack has formed , increases the magnitude of the stiffness matrix and enlarges the computational efforts required to solve the equilibrium equations for nodal

displacements. To overcome this difficulty two nodes occupying the same co-ordinates , connected by an infinite modulus spring linkage elements are defined. At the formation of the crack , the stiffness of the spring is brought to zero. When the shear effects of concrete after cracking are considered the springs of the linkage elements assume values for stiffnesses to reflect the effects of aggregate interlock and dowel action at the crack.

b. Smeared Cracking Model:

Many finely spaced cracks are assumed to form in a direction normal to the principal stress , when the principal stress exceeds the tensile strength of concrete. The concept of the smeared cracking model assumes not a displacement discontinuity but a stress discontinuity thereby allowing the automatic generation of cracks without a change in topology and a complete generality in the direction of cracks.

1.3.4 STEEL CONCRETE INTERFACE BEHAVIOR

The problem of describing and developing a model to reflect the steel concrete interface behavior is a very complicated three dimensional problem. So far , not enough experimental works were executed tofully understand the effects of interface behavior. The following is a summary of some of the experimental works carried out by researchers to study the

effect of bars bonded in a concrete matrix.

Broms(43) examined the locations , widths and extents of internal cracks of a concrete specimen reinforced with a single bar , with the aid of colored resins.

Gotto(44) used red ink and sawed the specimen to study the behavior of internal cracks. He observed many internal cracks of cone shapes with apex at bar lugs and base towards primary cracks. Most of the internal cracks made an angle of sixty degrees approximately to the bar axis. These comb-like internal cracks were formed due to the reaction exerted on concrete by the bar lugs as the steel stresses were increased. He also found that the steel stresses did not fall to zero even when the load was removed. This was attributed to the plastic deformation of the surrounding concrete.

Rehm(61) carried out series of pull-out tests and concluded that the slip between concrete and steel occurs by progressive crushing of concrete in front of bar lugs. He reported that approximately a length of six times the height of bar lugs , in front of a lug reaches the crushing stage.

Mirza and Houde(45) after an extensive experimental works showed that the crushing of concrete in front of bar lugs does not occur with the type of deformed bars used in practice. They sawed the specimen , found no marks or traces

of polishing on the concrete surface and the bar lugs stamped into the concrete firmly.Their findings lead them to conclude that noticable sliding or crushing of concrete does not seem to take place in front of the bar lugs.

1.3.5 POST CRACKING SHEAR BEHAVIOR

Post cracking shear behavior is usually accounted for by modifying the original shear modulus to a fraction of it's value , when a crack is formed in a smeared cracking model. The fraction was usually considered a constant or a function of the tensile strain normal to the crack , and was intended to account for the aggreate interlock and dowel mechanism that might be present .

Modification of the uncracked shear modulus , by a factor was first considered by Schnorbrich , Hand and Pecknold(33) They used a constant value of 0.4 for β for all stress and strain states in their non linear layered analysis of plates and shells.

Agrawal(34) used a constant value of 0.5 for β in the non linear analysis of concrete shear panels and deep coupling beams.

Cedolin and Dei-Poli(35) observed that a decreasing value for β predicted better responses for shallow beams failing in shear. They suggested the following reduced shear modulus

expression.

$\bar{G} = F(1.0 - \frac{\epsilon_1}{\epsilon_c})$ for $0 < \epsilon_1 < \epsilon_c$

$\bar{G} = 0.0$ for $\epsilon_1 > \epsilon_c$

where

$F = 0.1E$

ϵ_1 = strain normal to the crack

ϵ_c = limiting value of ϵ when the effect of aggregate interlock vanishes totally.

E = elastic modulus of concrete.

Al-Mahaidi(15) presented the following shear reduction expression for cracked concrete.

$\beta = 0.4/\frac{\epsilon_1}{\epsilon_{to}}$ for $\epsilon_1 > \epsilon_{to}$

$= 0.1$ for $\epsilon_1 < \epsilon_{to}$

where

= principal tensile strain normal to the crack.

= normal tensile strain at the formation of the crack.

Gilbert and Warner(28) used a value of 0.6 for β in the non linear analysis of reinforced concrete slab. They observed that the variation of β resulted in a negligible difference in the responses. They could not explain the insensitivity of in the slab responses.

1.3.6 TENSION STIFFENING EFFECT

Tension stiffening effect is usually taken into account for either by introducing a descending tensile stress-strain behavior for concrete or by modifying the steelstress-strain behavior.

Scanlon(39) proposed a descending tensile stress-strain behavior for concrete to account for the tension stiffening effect . He assumed that the tensile stress increases linearly up to the ultimate level and then suddenly the modulus of elasticity drops to the next lower level as shown in figure 4. The stress is now allowed to increase with the load to the limiting value corresponding to this branch of the diagram. This process is followed until the modulus of elasticity vanishes. By this process , the load carried by the steel gradually increases until it carries the entire load.

Lin and Scordelis(37) included the tension stiffening effect in the analysis of reinforced concrete shells of general form. The stress - strain curve suggested contained an elastic uncracked portion and a cracked unloading remainder. Once the concrete cracked , the tensile stress-strain curve assumed a following unloading curvilinear behavior.

$$\sigma = a_0 + a_1\epsilon + a_2\epsilon^2 + a_3\epsilon^3$$

The concrete was assumed to release it's entire stress at a strain of five times the cracking tensile strain. They also observed that the tension stiffening phenomenon has a significant effect on the response of member in the post cracking range but has little effects at the ultimate states.

Van Greunen(40) incorporated the tension stiffening effect by ignoring the contribution of concrete in carrying the tensile stress and increasing the elastic modulus of steel as shown in fig 6 . The additional stresses in the steel corresponds to the stress carried by the concrete. This method overestimates the steel stresses but underestimates the concrete stresses between the cracks.

Gilbert and Warner(38) considered the effects of different stress-strain behavior on the responses of their works. A value of ten times the cracking strain of concrete was assumed for , at which level the concrete stresses are totally released. The effect of modifying the steel stress-strain behavior was also considered , in their analysis of reinforced concrete slab. They found that modifying the steel stress-strain behavior to include the tension stiffening effect resulted in better responses and efficient use of computer time. They also concluded that the tension stiffening phenomenon has a significant effect on the deformation of the slab but showed negligible effect on the behavior at ultimate stress levels.

CHAPTER 2

FINITE ELEMENT MODEL FOR PLANAR STRUCTURES

2.1 INTRODUCTION

The stress-strain relationship of concrete, post-cracking behaviour modelling techniques, bond stress-slip relationships suggested by Houde(18) , which are presented in chapter 3, are all incorporated in the formulation of a finite element model for the nonlinear analysis of planar reinforced concrete members. Properties of finite elements used for idealisation of concrete and steel reinforcement are discussed. Modification of the stress-strain relationship of concrete due to cracking which is presented in chapter 3 is used in the present formulation of planar structures finite element model.

2.2 CONCRETE AND STEEL REPRESENTATION

2.2.1 LINEAR DISPLACEMENT QUADRILATERAL ELEMENT

The finite element used for the representation of concrete is shown in fig. 8 The element is a four node rectangle with two degrees of freedom at each node. The stiffness formulation of this element is well known and can be found in reference (47) . However , the stiffness formulation is repeated here for completeness and to explain the technique

of incorporating the incrementally non-linear stress-strain relationship discussed in section 3 into finite element model.

2.2.1.1 DISPLACEMENT FUNCTIONS

In order to make the integration required for the calculation of the stiffness matrix of the quadrilateral ring element practicable, the co-ordinate system ξ-η obtained by joining the midpoints of the opposite sides of the quadrilateral is used. Of course, the general quadrilateral maps into a square in the ξ-η plane.

Consider the single component of displacement δ_1. If the condition that all edges remain straight lines for the purpose of maintaining compatibility along the edges is enforced, then the displacement at any point (ξ,η) due to the diplacement δ_1 is given by

$u = (1/4)(1 - \xi)(1 - \eta)\delta_1$ and

$v = 0.0$

where u and v are the horizontal and vertical displacements respectively.

This may be repeated for both u and v for all possible nodal displacements as shown in figure 8 . By superimposing the equations for all possible nodal displacements and writing in

matrix form, one gets the following displacement formulas for points in the element when all eight nodal displacements are applied simultaneously.

$$\begin{bmatrix} u \\ v \end{bmatrix} = (0.25) \begin{bmatrix} kl & ml & mn & kn & 0 & 0 & 0 & 0 \\ 0 & 0 & 0 & 0 & kl & ml & mn & kn \end{bmatrix} \begin{bmatrix} \delta_1 \\ \delta_2 \\ \delta_3 \\ \delta_4 \\ \delta_5 \\ \delta_6 \\ \delta_7 \\ \delta_8 \end{bmatrix} \quad \text{.....2.1}$$

where

$k = 1 - \xi$

$l = 1 - \eta$

$m = 1 + \xi$

$n = 1 + \eta$

The functions k, l, m and n are called interpolation functions. They are also used to express the co-ordinate of any point (x , Y) in terms of the element nodal co-ordinates (X_1, Y_1), (X_2, Y_2), (X_3, Y_3) and (X_4, Y_4) as

$$\begin{bmatrix} X & Y \end{bmatrix} = (0.25) \begin{bmatrix} kl & ml & mn & kn \end{bmatrix} \begin{bmatrix} X_1 & Y_1 \\ X_2 & Y_2 \\ X_3 & Y_3 \\ X_4 & Y_4 \end{bmatrix} \quad \text{.....2.2}$$

2.3 STRAIN - DISPLACEMENT RELATIONSHIPS

The strain vector can be written as

$$[\epsilon] = \begin{bmatrix} \epsilon_{xx} \\ \epsilon_{yy} \\ \gamma_{xy} \end{bmatrix} = \begin{bmatrix} \frac{\partial}{\partial x} & 0 \\ 0 & \frac{\partial}{\partial y} \\ \frac{\partial}{\partial y} & \frac{\partial}{\partial x} \end{bmatrix} \begin{bmatrix} u \\ v \end{bmatrix} \quad \text{.....2.3}$$

Substitution of eqn.(2.1) into eqn.(2.3) gives

$$[\epsilon] = \frac{1}{4} \begin{bmatrix} \frac{\partial}{\partial x} & 0 \\ 0 & \frac{\partial}{\partial y} \\ \frac{\partial}{\partial y} & \frac{\partial}{\partial x} \end{bmatrix} \begin{bmatrix} kl & ml & mn & kn & 0 & 0 & 0 & 0 \\ 0 & 0 & 0 & 0 & kl & ml & mn & kn \end{bmatrix} \begin{bmatrix} \delta_1 \\ \delta_2 \\ \delta_3 \\ \delta_4 \\ \delta_5 \\ \delta_6 \\ \delta_7 \\ \delta_8 \end{bmatrix} \quad .2.4$$

or $[\epsilon] = [B][\delta]$

where $[B]$ is given by

$$[B] = (0.25) \begin{bmatrix} \frac{\partial}{\partial x} & 0 \\ 0 & \frac{\partial}{\partial y} \\ \frac{\partial}{\partial y} & \frac{\partial}{\partial x} \end{bmatrix} \begin{bmatrix} kl & ml & mn & kn & 0 & 0 & 0 & 0 \\ 0 & 0 & 0 & 0 & kl & ml & mn & kn \end{bmatrix} \quad \text{....2.5}$$

The differentiation of equation (2.5) cannot be performed directly as ξ and η cannnot be written as explicit functions of X and Y. Therefore, the chain rule of differentiation is used to carry out the differentiation,

$$\frac{\partial}{\partial \xi} = \frac{\partial x}{\partial \xi} \cdot \frac{\partial}{\partial x} + \frac{\partial y}{\partial \xi} \cdot \frac{\partial}{\partial y}$$

and

$$\frac{\partial}{\partial \eta} = \frac{\partial x}{\partial \eta}\cdot\frac{\partial}{\partial x} + \frac{\partial y}{\partial \eta}\cdot\frac{\partial}{\partial y}$$

or in the matrix form

$$\begin{bmatrix} \frac{\partial}{\partial \xi} \\ \frac{\partial}{\partial \eta} \end{bmatrix} = \begin{bmatrix} \frac{\partial x}{\partial \xi} & \frac{\partial y}{\partial \xi} \\ \frac{\partial x}{\partial \eta} & \frac{\partial y}{\partial \eta} \end{bmatrix} \begin{bmatrix} \frac{\partial}{\partial x} \\ \frac{\partial}{\partial y} \end{bmatrix} = [J] \begin{bmatrix} \frac{\partial}{\partial x} \\ \frac{\partial}{\partial y} \end{bmatrix} \quad \text{.....2.6}$$

where J is the Jacobian matrix, which can be evaluated by substitution from eqn.(2.2) , giving

$$[J] = (0.25) \begin{bmatrix} -l & l & n & -n \\ -k & -m & m & k \end{bmatrix} \begin{bmatrix} X_1 & Y_1 \\ X_2 & Y_2 \\ X_3 & Y_3 \\ X_4 & Y_4 \end{bmatrix} \quad \text{.....2.7}$$

At any point (ξ,η) in the element, the 2x2 $[J]$ matrix can be evaluated and inverted, putting

$$[J]^{-1} = [\bar{J}] = \begin{bmatrix} \bar{J}_{11} & \bar{J}_{12} \\ \bar{J}_{21} & \bar{J}_{22} \end{bmatrix}$$

Then from eqn. (2.6) , one gets

$$\begin{bmatrix} \frac{\partial}{\partial x} \\ \frac{\partial}{\partial y} \end{bmatrix} = [\bar{J}] \begin{bmatrix} \frac{\partial}{\partial \xi} \\ \frac{\partial}{\partial \eta} \end{bmatrix}$$

or

$$\frac{\partial}{\partial x} = \bar{J}_{11}\frac{\partial}{\partial \xi} + \bar{J}_{12}\frac{\partial}{\partial \eta}$$
$$\frac{\partial}{\partial y} = \bar{J}_{21}\frac{\partial}{\partial \xi} + \bar{J}_{22}\frac{\partial}{\partial \eta} \qquad \text{.....2.8}$$

Substitution of eqn.(2.8) into eqn.(2.5) gives

$$[B] = (0.25)\begin{bmatrix} \bar{J}_{11}\frac{\partial}{\partial \xi} + \bar{J}_{12}\frac{\partial}{\partial \eta} & 0 \\ 0 & \bar{J}_{21}\frac{\partial}{\partial \xi} + \bar{J}_{22}\frac{\partial}{\partial \eta} \\ \bar{J}_{21}\frac{\partial}{\partial \xi} + \bar{J}_{22}\frac{\partial}{\partial \eta} & \bar{J}_{11}\frac{\partial}{\partial \xi} + \bar{J}_{12}\frac{\partial}{\partial \eta} \end{bmatrix}$$
$$\begin{bmatrix} kl & ml & mn & kn & 0 & 0 & 0 & 0 \\ 0 & 0 & 0 & 0 & kl & ml & mn & kn \end{bmatrix}$$

In order to simplify the numerical integration , the matrix B is divided into two parts as follows;

$$[B] = [B_1] + [B_2]$$

where

$$[B_1] = \frac{1}{4}\begin{bmatrix} \bar{J}_{11} & 0 \\ 0 & \bar{J}_{21} \\ \bar{J}_{21} & \bar{J}_{11} \end{bmatrix} \begin{bmatrix} kl & ml & mn & kn & 0 & 0 & 0 & 0 \\ 0 & 0 & 0 & 0 & kl & ml & mn & kn \end{bmatrix}$$
.....2.9(a)

$$[B_2] = (0.25)\begin{bmatrix} \bar{J}_{12} & 0 \\ 0 & \bar{J}_{22} \\ \bar{J}_{22} & \bar{J}_{12} \end{bmatrix}\begin{bmatrix} kl & ml & mn & kn & 0 & 0 & 0 & 0 \\ 0 & 0 & 0 & 0 & kl & ml & mn & kn \end{bmatrix}$$
.....2.9(b)

Carrying out the differentiation in eqn.(2.9) gives:

$$[B_1] = (0.25)\begin{bmatrix} -l\bar{J}_{11} & l\bar{J}_{11} & n\bar{J}_{11} & -n\bar{J}_{11} & 0 & 0 & 0 & 0 \\ 0 & 0 & 0 & 0 & -l\bar{J}_{21} & l\bar{J}_{21} & n\bar{J}_{21} & -n\bar{J}_{21} \\ -l\bar{J}_{21} & l\bar{J}_{21} & n\bar{J}_{21} & -n\bar{J}_{21} & -l\bar{J}_{11} & l\bar{J}_{11} & n\bar{J}_{11} & -n\bar{J}_{11} \end{bmatrix}$$

and

$$[B_2] = (0.25)\begin{bmatrix} -k\bar{J}_{12} & -m\bar{J}_{12} & m\bar{J}_{12} & -k\bar{J}_{12} & 0 & 0 & 0 & 0 \\ 0 & 0 & 0 & 0 & -k\bar{J}_{22} & -m\bar{J}_{22} & m\bar{J}_{22} & k\bar{J}_{22} \\ -k\bar{J}_{21} & -m\bar{J}_{22} & m\bar{J}_{22} & -k\bar{J}_{22} & -k\bar{J}_{12} & -m\bar{J}_{12} & m\bar{J}_{12} & k\bar{J}_{12} \end{bmatrix}$$

2.4 STRESS-STRAIN RELATIONSHIP

The stresses and strains that contribute to strain energy of the element are those in the X-Y plane. The stress and strain vectors are

$$[\sigma] = \begin{bmatrix} \sigma_{xx} \\ \sigma_{yy} \\ \tau_{xy} \end{bmatrix} \qquad [\epsilon] = \begin{bmatrix} \epsilon_{xx} \\ \epsilon_{yy} \\ \gamma_{xy} \end{bmatrix} \quad \text{.....2.11}$$

For steel and concrete elements, the increment of stresses and strains are related by the relation

$$[\Delta\sigma] = [K_s][\Delta\epsilon] \quad \text{.....2.12}$$

where $[K_s]$ is given by

$$[K_s] = \frac{E\,(1-\nu)}{(1+\nu)(1-2\nu)}\begin{bmatrix} 1 & \frac{\nu}{1-\nu} & 0 \\ \frac{\nu}{1-\nu} & 1 & 0 \\ 0 & 0 & \frac{1-2\nu}{2(1-\nu)} \end{bmatrix}$$

where E is the young's modulus of steel or concrete(tangential) and ν is the poisson's ratio of steel or concrete.

2.5 FORMULATION OF ELEMENT STIFFNESS MATRIX

In the non-linear analysis, the load is applied in increments. Assuming that the application of an increment of load, $[\Delta P]$, to the nodes of the element results in increments of displacement $[\Delta\delta]$, strain $[\Delta\epsilon]$, and stress $[\Delta\sigma]$, respectively. The application of a small virtual nodal displacement $[\delta^*]$, produces additional strains at any point within the element $[\epsilon^*]$, which are given by:

$$[\epsilon^*] = [B][\delta^*] \qquad \text{.....2.13}$$

Assuming that the value of the small virtual nodal displacement is small enough such that the change in $[\delta^*]$ is negligible, the additional strain energy stored in the element during the virtual displacement can be written as :

$$\text{Increase in strain energy} = \int_{VOL} [\epsilon^*]^T [\Delta\sigma] \, dv$$
$$= \int_{VOL} [\delta^*]^T [B]^T [K_2] [\Delta\epsilon] \, dv$$
$$= \int_{VOL} [\delta^*]^T [B]^T [K_2] [B] [\Delta\delta] \, dv$$

The additional external work done by the nodal incremental load vector $[\Delta P]$is given by

$$\text{Additional external work} = [\delta^*]^T [\Delta P]$$

Equating the additional external work to the increase in strain energy gives

$$[\Delta P] = \int_{VOL.} [B]^T [K_g] [B] [\Delta\delta] \, dv \quad \ldots\ldots\ldots\ldots\ldots\ldots\ldots\ldots 2.14$$
$$= [K] [\Delta\delta]$$

where $[K]$, the element stiffness matrix, is given by

$$[K] = \int_{VOL.} [B]^T [K_g] [B] \, dv.$$

The above equation is used with four point Gauss numerical integration to obtain the element stiffness.

CHAPTER 3

FINITE ELEMENT ANALYSIS IN CONCRETE STRUCTURES

3.1 INTRODUCTION TO DISPLACEMENT FORMULATION

In many phases of engineering the solution of stress and strain distribution in elastic continua is required. The problems faced may range from two dimensional plane stress or plane strain distribution , axisymmetrical solids , plate bending and shells to fully three dimensional solids. In all cases the number of interconnections between any finite element isolated by some immaginary boundaries and the neighbouring elements is infinite. The problem of discretizing the above infinite connections is achieved through the followings.

(a) the continuum is separated by immaginary lines or surfaces into a number of finite elements.

(b) The elements are assumed to be interconnected at a discrete number of nodal points situated on their boundaries. The displacements of these nodal points will be the basic unknown parameters in the discrete structural analysis.

(c) A set of functions is chosen to define uniquely the state of displacement within each finite element in terms of its nodal displacements.

(d) The displacement functions now define uniquely the state of strain within an element in terms of the nodal displacements. These strains together with any initial strains and the constitutive properties of the material will define the state of stress throughout the element.

(e) A system of forces concentrated at the nodes and equilibrating the boundary stresses and any distributed loads is determined , resulting in a stiffness relationship.

Clearly a series of approximations has been introduced. Firstly , it is not always easy to ensure that the chosen displacement functions will satisfy the requirement of displacement continuity between adjacent elements. Thus the compatibility conditions on such interface lines may be violated. Secondly , by concentrating the equivalent forces at the nodes , equilibrium conditions are satisfied in the overall sense only. Local violation of equilibrium conditions within each element and on its boundaries will usually arise.

3.2 FINITE ELEMENT MESH

The choice of element shape for specific cases leaves much choice to the skills of the researcher or analyst. The degree of approximation which can be achieved obviously depends on the element shape assumed and the displacement function presumed.

Three different elements such as sub parametric , iso parametric and super-parametric elements are available for use in the finite element analysis. Out of these three available elements isoparametric elements are widely used.

Therefore in this thesis the computer program developed uses only isoparametric elements.

The use of triangular , rectangular and quadrilateral elements is common in the finite element analysis of reinforced concrete members. Using quadrilateral elements , reinforced concrete members , in general , can be modelled using a smaller number of elements than with the use of triangular or rectangular elements. Thus the choice of quadrilateral shape elements are preferred in this analysis.

3.3 PROPERTIES OF CROSS-SECTION

The analysis of reinforced concrete members is essentially a three dimensional problem. But when these members are subjected to in-plane loads only , the analysis can be reduced to a plane stress in nature , and the plane finite elements can be used to model the concrete and steel.

Consider a beam cross-section having the following properties.

The width of the section = b

Diameter of reinforcing bar = D

No. of reinforcing bar = m

The thickness of the concrete and steel elements which has the same space co-ordinates can be obtained by transforming the circular section of the reinforcing bar into a rectangular section. The following properties are used to determine the width and depth of the reinforcing bars of diameter D.

(a) The cross-sectional areas are equal.

(b) The moments of inertia remains same.

If b and h represent the equivalent rectangular sectional width and depth , then

$$\frac{\pi D^2}{4} = bh \quad \text{.....3.1}$$

$$\frac{\pi D^4}{64} = \frac{bh^3}{12} \quad \text{.....3.2}$$

The above equations yield to

$$b = \sqrt{3}D/2 \quad \text{.....3.3}$$

$$h = \pi D/2\sqrt{3} \quad \text{.....3.4}$$

3.4 CONSTITUTIVE RELATIONSHIP OF CONCRETE

A biaxial constitutive relationship and a suitable biaxial failure criterion is assumed in the present analysis when the concrete is subjected to a biaxial compressive stress state. When the stress state changes to purely tensile or only

compressive , then a uniaxial behaviour is considered.

3.4.1 BEHAVIOUR OF CONCRETE UNDER UNIAXIAL TENSION

The tensile strength of concrete is approximately ten percent of its compressive strength. But its contribution is usually neglected in practical designs.

The stress-strain curve is linear upto ninety percent ofthe failure load. This suggests that a linear curve can be assumed for concrete in tension without any serious errors resulting from this assumption.

3.4.2 BEHAVIOR OF CONCRETE UNDER UNIAXIAL COMPRESSION

The stress-strain curve is non linear under the action of uniaxial stress system. The parameters associated with the curve depends on many variables such as compressive strength , type of cement , coarse and fine aggregates , mix proportions , gradings of coarse and fine aggregates , water and cement ratio , size and shape of the testing specimen , the rate of loading and the age at loading etc.

Many proposals exist for the compressive stress-strain relationship , by many researchers and analysts. A review of these relationships are presented by Popovics(57).

Most of the proposed relations predict sufficiently closer

results in the elastic range. However ,considerable differences result in the descending branches after the maximum stress. It was also observed(57) that the stress-strain curves obtained from concentric compression and flexural specimens were not the same. The maximum strengths obtained from flexural stress system occured at much larger strains than obtained from uniaxial compressive stress system. Hence the use of most of the stress-strain curves obtained through uniaxial compressive stress state is conservative when applied to points in flexure.

Saenz's(5) proposed formula , provided below , is incorporated in the present analysis , for concrete subjected to compressive stress state.

$$\sigma = \frac{E\epsilon}{1 + (R + R_e - 2)\frac{\epsilon}{\epsilon_o} - (2R - 1)\left(\frac{\epsilon}{\epsilon_o}\right)^2 + R\left(\frac{\epsilon}{\epsilon_o}\right)^3} \qquad \ldots\ldots\ldots 3.5$$

where

$$R = \frac{R_e(R_f - 1) - 1}{(R_e - 1)\quad R_e}$$

$R_e = E/Es$

$R_f = \sigma_o/\sigma_f$

$Rc = \epsilon_f/\epsilon_o$

$Es = \sigma_o/\epsilon_o$

ϵ = strain

σ = stress

ϵ_o = strain corresponding to maximum stress

σ_o = maximum stress

ϵ_f = maximum strain at failure

σ_f = stress at failure

E = initial tangent modulus

Es = secant modulus

In the absense of any experimental values of ϵ_o and E , Saenz suggests the following formulii for their values.

$$\epsilon_o = 10^{-5} * 4\sqrt{f_c'}\ (31.5 - 4\sqrt{f_c'}) \quad \text{.....3.6}$$

$$E = 10^{5}\sqrt{f_c'} \ /\ (\ 1 + 0.006 f_c'\ ) \quad \text{.....3.7}$$

The differentiation of equation (3.5) will provide the necessary equation for the tangent modulus at any strain.

$$E_t = \frac{d\sigma}{d\epsilon} = \frac{E\ (\ 1 + C_1 (\frac{\epsilon}{\epsilon_o})^2 - 2C_2 (\frac{\epsilon}{\epsilon_o})^3\ )}{1 + C_3.\frac{\epsilon}{\epsilon_o} - C_1(\frac{\epsilon}{\epsilon_o})^2 + C_3.(\frac{\epsilon}{\epsilon_o})^3} \quad \text{.....3.8}$$

where

C1 = 2R-1

C2 = R

C3 = R+Re-2

3.4.3 BIAXIAL BEHAVIOR OF CONCRETE

In many occasions concrete is subjected to a tri - axial stress system. The displacement or deformation in any one direction is a function of the applied stresses and

deformations of all three directions. However , usually triaxial effect is not too significant in all three directions , and the use of biaxial stress system closely predicts the behavior of the member considered. Reinforced concrete exhibits a higher ultimate loads when subjected to biaxial stress system , thereby necessitating the use of biaxial behavior of concrete in case of a more accurate analysis.

The stress-strain relation in a biaxial stress state is expressed by the following formula

$$\sigma = \epsilon E / (1 - \nu\alpha) \qquad \text{.....3.9}$$

where

σ = stress in the direction considered

ϵ = strain in the direction considered

α = ratio of the principal stress in the direction orthogonal to the principal stress direction considered

E = initial tangent modulus in uniaxial stress system

ν = Poisson's ratio in uniaxial stress system

Liu , Nilson et al(12) suggested a non linear stress-strain relationship under biaxial compressive stress state.

$$\sigma = \frac{\epsilon E}{(1-\nu\alpha)\left[1+\left(\frac{E}{\sigma_p(1-\nu\alpha)}-\frac{2}{\epsilon_p}\right)\epsilon+\left(\frac{\epsilon}{\epsilon_p}\right)^2\right]} \qquad \text{..3.10}$$

where

σ_p = the ultimate strength of concrete under biaxial compression

ϵ_p = the strain at maximum stress for concrete under biaxial compression

σ can be written in the following form also ,

$$\sigma = \frac{\epsilon E}{(1-2\nu)\left[1+\left(\frac{1}{1-2\nu}\cdot\frac{E}{E_s}-2\right)\frac{\epsilon}{\epsilon_p}+\left(\frac{\epsilon}{\epsilon_p}\right)^2\right]} \qquad ..3.11$$

$E_s = \frac{\sigma_p}{\epsilon_p}$ = secant modulus at ultimate laod.

It is best to use experimentally obtained values for modulus of elasticity and Poisson's ratio. In the absense of such datas , the following values may be assumed in the uniaxial stress system.

Poisson's ratio $\nu = 0.2$

$$E = 33w^{\frac{3}{2}}\sqrt{f_c'} \qquad .....3.12$$

where

w = unit weight of concrete in lbs. per cu.ft.

f_c' = ultimate cylinder strength of the concrete in uniaxial compression in psi.

Based on Liu(26)'s experimental datas and results Liu and Nilson (12) put forward the following expressions for the calculation of ultimate strength σ_p and strain ϵ_p at maximum stress of concrete under biaxial compression.

$\alpha < 0.2$ $= (1 + \alpha / (1.2 - \alpha))$ .....3.13(a)

$0.2 \leq \alpha \leq 1.0$ $= 1.2 \sigma_0$ .....3.13(b)

$1.0 \leq \alpha \leq 5.0$ $= 1.2 \sigma_0 / \alpha$ .....3.13(c)

$\alpha > 5.0$ $= \frac{1}{\alpha} (1 + 1 / (1.2\alpha - 1))$ .....3.13(d)

σ_0 = ultimate strength of concrete in uniaxial compression.

and

$\alpha \leq 1.0$ $\varepsilon_p = 0.0025$

$\alpha > 1.0$ $\varepsilon_p = (-500 + 0.55\sigma_p) \times 10^{-6}$

where

σ_p = Larger principal stress in psi.

3.4.4 ORTHOTROPIC STRESS-STRAIN RELATIONS

The constitutive equations for an orthotropic elastic material under biaxial compression will assume a following form.

$$\begin{bmatrix} \sigma_1 \\ \sigma_2 \\ \sigma_3 \end{bmatrix} = \begin{bmatrix} \lambda_1 & \lambda\nu_1 & 0 \\ \lambda\nu_1 & \lambda E_2/E_1 & 0 \\ 0 & 0 & \dfrac{E_1 E_2}{E_1 + E_2 + 2E_2\nu_1} \end{bmatrix} \underline{\varepsilon} \quad \text{.....3.14}$$

where

E_1, E_2 = the uniaxial tangential modulus in the directions 1,2 respectively

ν_1, ν_2 = Poisson's ratios of concrete in the directions 1,2 respectively.

$$\lambda = \frac{E_2}{\frac{E_2}{E_1} - \nu_1^2} = \frac{E_1}{1 - \frac{E_1}{E_2}\nu_1^2} \qquad \text{.....3.15}$$

In the derivation of eqn. (3.14) it was assumed that the stiffness in perpendicular directions are caused only by poisson's effect. The experimental results show higher values of stiffnesses in perpendicular directions if poisson's effect alone is considered under a biaxial state of stress. The concrete confinement is the prime cause for the additional stiffness.

To account for the concrete confinement , effective tangent modulii have to be calculated and used in an uncoupled form of the constitutive relationship.

$$\begin{bmatrix} \sigma_1 \\ \sigma_2 \\ \sigma_3 \end{bmatrix} = \begin{bmatrix} E_{1b} & 0 & 0 \\ 0 & E_{2b} & 0 \\ 0 & 0 & G_b \end{bmatrix} \begin{bmatrix} \epsilon_1 \\ \epsilon_2 \\ \epsilon_{12} \end{bmatrix} \qquad \text{.....3.16}$$

where

E_{1b} , E_{2b} = effective tangent modulii in directions 1 and 2.

G_b = shear modulus for biaxially stressed concrete.

Differentiation of eqn. (3.11) yields

$$E_b = \frac{d\sigma}{d\epsilon} = \frac{E\left(1 - \left(\frac{\epsilon}{\epsilon_p}\right)^2\right)}{(1-\nu\alpha)\left[1 + \left(\frac{1}{1-\nu\alpha}\cdot\frac{E}{E_s} - 2\right)\frac{\epsilon}{\epsilon_p} + \left(\frac{\epsilon}{\epsilon_p}\right)^2\right]^2} \qquad \text{....3.17}$$

Eqn.(3.17) can be written to separate the poisson's effect from concrete confinement.

$$E_b = \frac{E_b'}{1-2\nu\alpha} \qquad \text{.....3.18}$$

where

$$E_b' = \frac{E\left[1-\left(\frac{\epsilon}{\epsilon_p}\right)^2\right]}{(1-2\nu\alpha)\left[1+\left(\frac{1}{1-2\nu\alpha}\cdot\frac{E}{E_s}-2\right)\frac{\epsilon}{\epsilon_p}+\left(\frac{\epsilon}{\epsilon_p}\right)^2\right]^2} \qquad \text{.....3.19}$$

Now the constitutive eqn. of the biaxially stressed concrete can be expressed , similar to eqn.(3.11) as

$$\begin{bmatrix}\sigma_1\\ \sigma_2\\ \sigma_3\end{bmatrix} = \begin{bmatrix}\lambda' & \lambda'\nu_1 & 0\\ \lambda'\nu_1 & \frac{\lambda' E_{2b}'}{E_{1b}'} & 0\\ 0 & 0 & \frac{E_{1b}'\cdot E_{2b}'}{E_{1b}'+E_{2b}'+2E_{2b}'\cdot\nu_1}\end{bmatrix}\begin{bmatrix}\epsilon_1\\ \epsilon_2\\ \epsilon_3\end{bmatrix} \qquad \text{.....3.20}$$

where

$$\lambda' = \frac{E_{2b}'}{\frac{E_{2b}'}{E_{1b}'}-\nu_1-2} \qquad \text{.....3.21}$$

with E_{1b}' and E_{2b}' obtained replacing ϵ by ϵ_1 and ϵ_2 in eqn. (3.19).

Eqn.(3.20) can be used for biaxial tension and tension compression cases by simply replacing E1b' , E2b' with the suitable tangent modulii.

3.4.5 PROPERTIES OF STEEL

Reinforced steel is usually present in the form of slender bars in most reinforced concrete members. As a result we need to take only the uniaxial tension or uniaxial compression in the failure state. Biaxial state of stress can be ignored in these circumstances.

The present analysis assumes the following simplified stress-strain relationship expressed in fig 14 .

Beyond the yield point , the tangent modulus is zero. However , a small value is assigned to it to eliminate any possibility of the occurance of singularity and is assumed to have a value equal to the initial strain hardening modulus when the principal strain exceeds the strain hardening limit.

3.4.6 FAILURE CRITERION OF CONCRETE

There exist many different failure criterions such as the maximum principal stress or strain criteria , maximum shear stress criteria , internal friction , volumetric stress modification criteria etc.

When the concrete fails under uniaxial or biaxial compression , the maximum principal strain theory for compressive failure criteria looks reasonable and its application is straight forward. For uniaxial tensile stress failure , the maximum

principal stress theory seems more suitable. These two failure criterions are employed in the present analysis.

The maximum stress theory implies that the failure occurs when the maximum principal stress reaches the uniaxial strength at failure. This theory agrees very well with the tensile failure but the results don't tally when applied to uniaxial or biaxial compression failure. When the tensile strength criterion was applied to flexural members , the experimental data gave a conservative result.

It was also observed that high tensile strain gradients exist in the tension zone. Therefore it could be concluded that the choice of modulus of rupture of concrete f presents realistic values than uniaxial tensile strength criterion. The value of f_r could be evaluated using the following expression.

$$f_r = 0.008f'_c + 280 \quad \text{(psi.)} \quad \ldots\ldots\ldots\ldots\ldots\ldots 3.22$$

The maximum strain theory implies that the concrete fails in compression when it reaches an ultimate strain of 0.003 in/in.This value is true only in the case of uniaxial compression. Under the action of biaxial stress state the limiting strain is affected by the principal stress. When the principal stress ratio becomes larger (> 0.5) the limiting strain value is considerably reduced. It may be concluded

from the above reasoning that the use of single ultimate strain would not be the best choice as the failure criterion of concrete.

3.5 STEEL CONCRETE INTERFACE BEHAVIOR

3.5.1 FORCES AT INTERFACE

The bond stress is defined as the shearing force acting around the circumference of the bar parallel to its longitudinal axis. In the case of a deformed bar , nominal diameter is considered in the calculation of the bond stress. Adhesion and friction contributes to the bond stress in the plain bars. Usually the slip between the concrete and steel along the interface is very much considerable.

Adhesion and friction are of secondary importance in the contribution of bond stresses in the deformed bars. The compressive reactions on the lugs exerted by the concrete contributes a major portion in providing the bond stresses. These compressive forces create the shear stresses on the outer surface of the concrete sheath which fills the space between the lugs. The radial component of the reaction at the lugs significantly increases the bond resistance.

During the early stages of loading , very little slip or no slip occurs between the steel and the concrete. As the load is increased the cracking and breaking of bond causes the

slip to become large. The longitudinal bars , in the meantime , prevent any sliding movement of the cracked surfaces causing a dowel action mechanism to occur.

Ngo and Scordelis used a special type of element called " Linkage Element " to portray the interface effects. Linkage elements have no physical size.It is introduced in between steel and concrete nodes where they occupy the same positions in the space. The linkage element comprises of two orthogonal springs with the longitudinal spring simulating the bond stress-slip action and the transverse spring modelling the dowell action mechanism. The horizontal and vertical stiffnesses of these springs are functions of the type of concrete , the amount of concrete cover , bar type and dimensions and the bar spacing.

The dowel action mechanism and the bond stress-slip behavior are interconnected. Because of lack of experimental works and datas on this area it looks at this stage to consider these two effects uncoupled. Therefore in the present analysis much attention is given to bond stress-slip phenomenon and the dowel action is simplified by assigning a constant arbitrary value to it.

3.5.2 STIFFNESS OF LINKAGE ELEMENT

The following expression represents the relationship between

the spring forces and the spring deformations.

$$\underline{F} = \underline{k}\underline{d} \quad \text{.....3.23}$$

where

$\underline{k}$ = spring stiffness matrix

$\underline{d}$ = spring deformation vector

$\underline{F}$ = spring force vector

The deformation vector consists of two components , first being the bond slip measurement for the longitudinal spring and the second being the dowel displacement value for the transverse spring.

The following expression evaluates the deformation vector.

$$\underline{d} = \underline{d}_S - \underline{d}_C$$

where

$\underline{d}_S$ = displacements of the steel node

$\underline{d}_C$ = displacements of the concrete node

In the matrix form the bond force , deformation can be written as

$$\begin{bmatrix} F_H \\ F_V \end{bmatrix} = \begin{bmatrix} K_H & 0 \\ 0 & K_V \end{bmatrix} \begin{bmatrix} d_H \\ d_V \end{bmatrix} \quad \text{.....3.24}$$

where

F_H = horizontal spring force

F_V = vertical spring force

d_H = horizontal spring deformation

d_V = vertical spring deformation

K_H = horizontal spring stiffness

K_V = vertical spring stiffness

Let assume that the co-ordinate axes of the spring makes an angle θ with the global co-ordinate axis system , then

$$\begin{bmatrix} F_{1x} \\ F_{1y} \\ F_{2x} \\ F_{2y} \end{bmatrix} = \begin{bmatrix} -c & s \\ -s & c \\ c & -s \\ s & c \end{bmatrix} \begin{bmatrix} F_H \\ F_V \end{bmatrix} \quad \text{.....3.25}$$

where

$c = \cos\theta$

$s = \sin\theta$

F_{ix}, F_{iy} are the force components at node i in the global axes system.

Similarly

$$\begin{bmatrix} d_H \\ d_V \end{bmatrix} = \begin{bmatrix} -c & -s & c & s \\ s & -c & -s & c \end{bmatrix} \begin{bmatrix} d_{1x} \\ d_{1y} \\ d_{2x} \\ d_{2y} \end{bmatrix} \quad \text{.....3.26}$$

where

d_{ix}, d_{iy} = displacement components of node i.

The global stiffness matrix of the linkage element can be

obtained by combining eqns. (3.24),(3.25) and (3.26).

$$\underline{K} = \begin{bmatrix} -c & s \\ -s & -c \\ c & -s \\ s & c \end{bmatrix} \begin{bmatrix} k_V & 0 \\ 0 & k_H \end{bmatrix} \begin{bmatrix} -c & -s & c & s \\ s & -c & -s & c \end{bmatrix} \quad \text{.....3.27}$$

k_V and k_H are the tangential modulus values of the non linear bond stress - slip , dowel - deformation relationships.

3.5.3 BOND STRESS-SLIP RELATIONSHIPS

A typical bond stress-slip relationship is shown in fig 16 . After the occurance of maximum bond stress the curve divides into two different parts. The bond stress remains essentially constant for an interior bonding area. The formation of longitudinal crack between the bar and the concrete cover in an exterior bonding area causes the bond stress to fall to zero.

Bressler and Berto(62) carried out tests on an axially loaded specimen at a load level of 32 psi at the protruding ends of the bar. Nilson , using these experimental datas and the method of least squares,suggested the following third degree polynomial relationships between bond stress and slip.

$$u = 3.606*10^{6}d - 5.356*10^{9}d^{2} + 1.936*10^{12}d^{3} \quad \text{....3.28}$$

The incremental tangential modulus is obtained by the

differentiation of eqn.(3.28).

$$du/dd = 3.606*10^{6} - 10.712*10^{9}d + 5.936*10^{12}d^{2} \quad ..3.29$$

where

u = local bond stress in psi.

d = local bond slip in 10^{-6} in.

Houde and Mirza tested a large number of concentric tensile specimens and beam ends of different sizes which were reinforced with steel bars of varying diameter. They also considered the effects of concrete strength , steel stress levels and came out with the following expression.

$$u = 1.95*10^{6}d - 2.35*10^{9}d^{2} + 1.39*10^{12}d^{3} - 0.33*10^{15}d^{4} .....3.30$$

The differentiation of eqn. (3.30) provides the necessary incremental stiffness of the longitudinal spring.

$$du/dd = 1.95*10^{6} - 4.70*10^{9}d + 4.17*10^{12}d^{2} - 1.32*10^{15}d^{3} \quad ..3.31$$

The initial spring stiffness is obtained by the substitution of d = 0 in eqn.(3.31) and has a value of approximately 2.0 psi/in. This value agrees with the experimental values obtained by Nilson.

The bond stress-slip relationship expressed by eqn. (3.30) is valid for a concrete strength of 5000 psi.. Different concrete strengths are incorporated in the expression by

using a multiplier ($f'_c/5000)^{1/2}$.

The longitudinal stiffness of a spring in a particular cross-section is evaluated by

k_H = du/dd*m*L*D 3.32

where

m = the number of bars in the cross-section

L = the length over which each spring acts

D = diameter of the bar

In an incremental approach , adopted in the present analysis , a larger increment could generate an increased spring stiffness. The spring stiffness can be brought to theoritical values only if the increments are kept small , leaving an uneconomical procedure. Instead Nilson proposed an average stiffness for use in an increment. The average stiffness is calculated by predicting a new slip value for the next loading step. That is

$d_{n+1}=d_n+c(d_n-d_{n-1})$ 3.31

where

d_{n+1}= the value of slip at the end of loading step n+1

d_n = the value of slip at the end of loading step n

d_{n-1}= the value of slip at the end of loading step n-1

c = constant.

The assumption of 0.7 for c provides better results(48,50).

3.5.4 BOND FAILURE CRITERIA

From the bond stress-slip curve shown in fig 16 one can observe that after a specific slip value, the curve starts to descend giving a negative gradient. Therefore a limiting value of slip must be enforced to avoid any computational difficulties associated with the negative slopes.

Splitting failures dominate in most of the bond failures in concrete when reinforced with deformed bars. As the loads are increased oblique cracks making more than 45 degrees with the longitudinal bar axis are formed in the concrete. These cracks generate from the tip of the lugs and spread towards the main crack forming hollow truncated cones around the bar. Experimental observation shows that the radial forces are much greater than the bond stress values. These greater radial forces burst the surrounding concrete.

Two different failure criterias are developed for link elements depending on their locations. Near the open faces the confinement of concrete is little but high splitting forces act on those regions. As a result a wedge of the concrete is pulled out and the relative movement of the steel and concrete far exceeds the limiting bond slip value with the associated spring stiffnesses falling to zero. When a steel element lies far away from the open face, the confinement prevents the growth of inclined cracks and the

early formation of wide cracks. Even after the bond slip exceeds the limiting value, the concrete is capable of sustaining the forces exerted by the lugs. Therefore the interior springs remain active even after the limiting slip value but fails totally after the formation of wide cracks.

3.5.5 DOWEL ACTION

Once a crack is formed, the shear force across a crack is transmitted by the uncracked concrete section, aggregate interlock of cracked portion and the dowel action. The contribution of the dowel action becomes predominant when the crack width increases and the relative movement of the cracked surfaces is measurable.

The surrounding concrete exerts compressive or tensile forces on the bar perpendicular to the bar axis. The distribution of these forces are shown in fig 19 . The dowel springs representing the dowel actions will exhibit different behaviour depending on whether they are located in the tension zone or compression zone. Those springs in the tension area represents the normal forces created mainly by the adhesion between steel and concrete. Houde and Mirza(54) approximated the normal tension behaviour by a linear tensile stress-strain behaviour of the concret cover.

The presence of stirrups , position of reinforced bars and

geometry of the cross-section usually affects the behaviour of compression springs denoted as C_i and C_e in fig 19 . The springs situated inside the member are generally stiff, but their exact behaviour is not understood thus necessitating the use of an approximation. The assumption of a constant spring stiffness value may be a good start for the analysis. Ngo and Scordelis(3) employed high values for their analysis. Nilson (48) observed that the use of high values prevents the formation of longitudinal cracks in concrete in the computer model. The observation lead him to use a low value at the start and eventually reducing that to zero.

The concrete in the cover matrix is not bound by any reinforcement and therefore is usually weak. Early splitting failure of the concrete in the cover area reduces the stiffness of the dowel springs connected to the cover concrete.

Dowel action behaviour can be analysed by using the finite element method. Since the present analysis considers the general overall analysis of the structural member, simple assumptions of the dowel springs are considered. A low constant stiffness value is assumed for internal and cover dowel springs.

3.6 STIRRUPS

Stirrups enclose over 90 % of concrete in a structural member. This enclosure creating a confining effect increases the compressive strength and shear strength of the concrete. Very less effort was rendered towards the effect of stirrups than the main reinforcement by many researchers. As a result of lack of data it is very difficult to model the concrete stirrup interaction.

Stirrups transfer the shear forces mainly through developing axial forces in it. Therefore the dowel spring effect associated with any reinforcement can be ignored. The interaction may then be represented by only longitudinal bond spring elements acting parallel to the stirrup axis.

The inclusion of longitudinal bond spring elements increase the number of nodes. When the primary forces in a member are of shear nature, this method of modelling the stirrup concrete interaction could be recommended. The use of this method requires a suitable mesh configuration. When a general analysis is performed further simplifications seem logical. The present analysis considers only the general behaviour and therefore the following considerably easier representation is made.

The stirrup is represented by a four degree of freedom bar

elements, not associated with bond or dowel springs. Lets assume that the axis of the bar element make an angle θ with the global axis. In the local co-ordinate system the stiffness of the bar element is given by the following matrix.

$$k_b = \begin{bmatrix} A_s E_s/L_s & -A_s E_s/L_s \\ -A_s E_s/L_s & A_s E_s/L_s \end{bmatrix} \quad \text{.....3.32}$$

If represents the relevent transformation matrix, the stiffness matrix in the global system $\underline{K}_b$ can be obtained by the following equation.

$$\underline{K}_b = \underline{\lambda}^T \underline{k}_b \underline{\lambda}$$

$$\underline{K}_b = \begin{bmatrix} c & 0 \\ s & 0 \\ 0 & c \\ 0 & s \end{bmatrix} \begin{bmatrix} A_s E_s/L_s & -A_s E_s/L_s \\ -A_s E_s/L_s & A_s E_s/L_s \end{bmatrix} \begin{bmatrix} c & s & 0 & 0 \\ 0 & 0 & c & s \end{bmatrix}$$

.....3.33

where

A_s = cross-sectional area of the stirrup.

E_s = modulus of elasticity of stirrup.

$c = \cos\theta$

$s = \sin\theta$

The above equation provides the following stiffness matrix for the stirrup bar,

$$K = \left[A_S E_S / L_S\right] \begin{bmatrix} c^2 & cs & -c^2 & -cs \\ cs & s^2 & cs & -s^2 \\ c^2 & cs & c^2 & cs \\ -cs & -s^2 & cs & s^2 \end{bmatrix} \quad \ldots\ldots\ldots\ldots\ldots\ldots 3.34$$

The location of the bar elements can be in between any two steel nodes, or concrete nodes or steel and concrete node as shown in fig 21.

Under the action of a stress system, the stirrups transfer stresses to the surrounding concrete. When the concrete is uncracked, however , the stresses in the stirrup are not as high as in a bar element undergoing the two displacements at the ends only. Moreover a bar element having one node at the upper steel element and the other node at the lower steel element can create an arbitrary truss-like rigidity. Therefore it would be advisable to idealise a stirrup through a few bar elements connected to interior concrete nodes. This idealisation would provide improved behaviour in the computer model.

3.7 CRACKING

Many microcracks exist in the concrete even before any external load is applied to the concrete. The failure criterion consisting of the stresses and strains associated with single microcrack is very hard to formulate. The use of

energy concepts of failure mechanism has been proposed by Kaplan(65).

When an external load is applied to the concrete energy is absorbed through elastic deformation and in the formation and propagation of the microcracks. Irwin(66) considers the strain energy release rate is directly connected with the propagation of microcracks and measures the stress level surrounding the crack.

In the finite element analysis once the failure of the concrete element occured , the strain energy stored in the element is released and is assumed to be redistributed into the remaining structure. The energy level, therefore, may rise in the surrounding elements sharply causing some new elements to crack under the same load.

Consider the effects at loading step n. Let the nodal forces and the nodal displacements of the element at loading step n be represented by P_n and D_{en} respectively. For equilibrium of the uncracked element,

$P_n=K*D_{en}$ 3.35

where

K= the stiffness matrix of the uncracked element at the end of the loading step n.

P_n, D_{en} = element nodal force vector and element displacement

vector at the end of loading step n.

If an element cracks at the end of the loading step n, the original element stiffness is reduced to a lower stiffness matrix denoted by $\underline{K}_n^r$. Then the nodal forces $\underline{P}_n^r$ that could be allowed with the associated stiffness matrix K_n^r is given by the following equation,

$$\underline{P}_n^r = \underline{K}_n^r * \underline{D}_{en} \quad \text{.....3.36}$$

The difference between the two nodal forces will be redistributed in the n+1 loading step.

$$\underline{P}_{n+1}^F = \underline{P}_n - \underline{P}_n^r = (\underline{K}_n - \underline{K}_n^r) * \underline{D}_{en} \quad \text{.....3.37}$$

where

$\underline{P}_{n+1}^F$ = redistributed load vector to be redistributed inthe n+1 loading step.

In a given loading step released nodal force vectors Pn will form another self-equilibrating force system . This additional force system will be included in the n+1 loading step nodal forces $\underline{P}_{n+1}$. During a loading step if these redistributed nodal forces create additional elements to crack, the crack pattern is called an unstable crack. By using an iterative technique in a loading step, the structure can be reanalysed to obtain a stable crack pattern. In otherwords the iterative process within each loading is terminated until a a new structure stiffness is formed which

causes no new elements to crack.

The iterative technique within a loading step seems costly in the computer time and could be avoided if small load increments are assumed in the loading process. Under small load increments, the number of elements cracking in that particular loading step is small. Thus the redistributed forces could effect only small changes in the stress field.

When an element cracks it looses its stiffness perpendicular to the crack, but resists the forces parallel to the crack. The direction of the crack is given by the principal stress directions representing the failure stress values. The formation of the crack also changes the material property of the concrete from isotropic to orthotropic.

If the direction 1 is always assumed to be perpendicular to the crack direction then the elastic modulus $E_1 = 0$. After the crack is formed, and the associated elasticity matrix is given by the following matrix.

$$E = \begin{bmatrix} 0 & 0 & 0 \\ 0 & E_2 & 0 \\ 0 & 0 & 0 \end{bmatrix} \qquad \text{.....3.38}$$

Obviously this is in the element crack direction co-ordinate system. Using the transformation, the cracked element stiffness is obtained as the following matrix in the global

system.

$$E = E_2 \begin{bmatrix} s^4 & s^2c^2 & -s^3c \\ s^2c^2 & c^4 & -sc^3 \\ -s^3c & -sc^3 & s^2c^2 \end{bmatrix} \quad \text{.....3.39}$$

A similar approach is adopted in the treatment of the crushed concrete elements. When the greater principal strain reaches an ultimate value of 0.003, a failurre direction is defined by the corresponding principal direction. The crushed concrete element is able to transfer stresses in a direction parallel to this principal direction, but unable to transfer forces perpendicular to this principal direction.

CHAPTER 4

ANALYSIS OF RESULTS

4.1 INTRODUCTION

The computer program used (the input can be found in the appendix) has the following capabilities.

(1) Simulate the cracking of concrete without eliminating the cracked elements from the member.

(2) Utilise the increase of compressive strength of concrete under biaxial stress state.

This program was used to analyse one singly reinforced and one doubly reinforced simply supported beam for the entire loading history from zero until failure.

4.2 SINGLY REINFORCED SIMPLY SUPPORTED BEAM

4.2.1 DESCRIPTION

The beam has a width of 12 inches , depth of 20 in. and is reinforced with 2#9 bottom bars. The ultimate strength of concrete is 4000 psi and the reinforcing steel has a yield strength of 40000psi. The total length of the beam is 130 in.The beam is loaded by two point loads each of which is situated 21 in. from the midspan (Fig.22).

Since the beam is symmetrical about the vertical centerline, one half of the beam is analysed.The concrete mass is divided

into 88 rectangular elements.The reinforcing steel bar is represented by 11 rectangular steel elements. 24 link elements are introduced in between the respective concrete and steel nodes. The beam has 120 nodes and each node has 2 degrees of freedom. The circular cross-section of the bars are transformed to equivalent rectangular sections using the formulae presented in section 3.2. The input data are reduced to a beam of unit width.

4.2.2 INTERPRETATION OF RESULTS

Choice of loading increments affectsthe finite element analysis of reinforced concrete structures. Larger load increments tend to create divergence, whereas smaller increments increase the computer time and of course the cost of the analysis. Numerous trial runs were made to obtain the end of elastic range and the associated applied load(1120lb).

The loading increments of 100 lb. was set after the application of the initial load which terminates the elastic range. Before any load increment is applied to the structure, a stability check is made to ensure that new cracks do not form as the nodal forces are redistributed. This procedure was repeated until the failure state of the beam is reached. The following observations were made from the computer output and the load deflection curve and bond force distributions are plotted.

4.2.2.1 ELASTIC RANGE OF LOADING

1. Concrete, steel stresses, bond stresses and deflection obtained for the initial load of 1120 lb. assume elastic properties of the beam and therefore correspond to the elastic range of the beam behaviour. The redistribution of nodal forces of the cracked elements and the nonlinear behaviour of concrete are taken into consideration in the subsequent application of load increments.

2. The longitudinal concrete stress and the associated longitudinal strain vary linearly across the cross-section.

3. The shear stress distribution across the cross-section varies parabolically and agrees well with the elastic theory.

4. Maximum shear stress values are observed at the supports.

5. A gradual increase in longitudinal steel stresses are observed as we move from the support to the center of the beam. The longitudinal stress values are almost same in the constant moment zone area.

6. The bond force between steel and concrete is very small in all the steel elements. The assumption of perfect bond between steel and concrete in the elastic range seems reasonable.

7. The deflection of the beam at midspan is 0.0349 in. which

is close to the computed value given in reference 17(0.0355).

4.2.2.2 CRACK INITIATION AND PROPAGATION

1. One primary crack is formed in the element 73 inside the constant moment zone at a load of 1120 lb. The principal tensile stress in the concrete elements next to the steel elements are close to the modulous of rupture which has a value of 650 psi.

2. As the applied load increases the crack propagates upward and at a load level of 1220 lb. Three additional cracks appear in the adjacent elements.

3. As additional elements crack the tensile stresses previously carried by these elements are now transferred to steel and the steel stresses increase significantly. The increase is almost 100% at the load level of 1420 lb. as compared to the values at a load level of 1120 lb.

4. As the crack propagates towards the compression zone, the principal tensile stresses of the concrete elements at the tip of the cracked elements decrease.

At 1120 lb. f_t = 416 psi.

At 1320 lb. f_t = 345 psi.

5.The strain in the uncracked concrete elements which lies in between the cracked elements decrease compared to the values

they achieved at the elastic range.

6. The shear stresses in the concrete increase as the load increases and with the crack propagating upwards. At 1420 lb. the concrete shear stresses increase by 30% in the uncracked zone with respect to the values corresponding to the initial load. The remaining shear stresses carried by the cracked elements are very small.

7. In the elastic range , approximately 2% of the shear is carried by the steel element. As the crack forms, this value increases to nearly 10%.

8. A significant increase in bond forces are observed around the cracks. The bond forces have an average value of 50 psi at 1120 lb. applied load. At the first crack under the load level of 1220 lb. the bond force is increased to 300 lb., whereas the corresponding value in the uncracked vicinity is only 35 lb.

9. A better co-relation between the longitudinal steel stresses and the crack pattern is visible at a load level of 1620 lb. High steel stresses occur at the crack and lower stresses result in between the cracks. The steel stresses are evenly distributed with high values at the cracks and slightly lower values in between the cracks as the failure load is approached.

10. Bond link elements fail at the high steel stress locations.

4.3 DOUBLY REINFORCED SIMPLY SUPPORTED BEAM

4.3.1 DESCRIPTION

The beam has a width of 6 in., depth of 12 in. and is reinforced with 2#6 bottom bars and 2#4 top bars. The ultimate strength of the concrete is 4000 psi and the reinforcing steel has a yield strength of 40000 psi. The total length of the beam is 120 in. The beam is loaded by two point loads each of which is situated 18 in. from the midspan (Fig.27).

Since the beam is symmetrical about the vertical centerline, one half of the beam is analysed. The concrete is divided into 100 rectangular elements. The reinforcing steel bar is represented by 20 rectangular steel elements. 40 link elements are introduced in between the respective concrete and steel nodes. The beam has 143 nodes and each node accomodates 2 degrees of freedom. The circular reinforcing bars are transformed to equivalent rectangular sections using the formulii presented in section 3.2. The input datas are reduced to a beam of unit width.

4.3.2 INTERPRETATION OF RESULTS

4.3.2.1 ELASTIC RANGE OF LOADING

1. Concrete stresses, steel stresses and deflections obtained for the initial load of 580 lb. assume elastic properties of the beam and therefore corresponds to the elastic range of the beam behavior. The redistribution of nodal forces of the cracked elements and the nonlinear behavior of concrete are taken into consideration in the subsequent application of load increments.

2. The longitudinal concrete stress and the strain vary linearly across a section.

3. The shear stress distribution across the cross-section varies parabolically thus agrees well with the elastic theory.

4. Maximum shear stresses appear near the supports.

5. A gradual increase in the longitudinal steel stresses are noted from the support to the center of the beam. The longitudinal stresses approach a constant value in the constant moment zone.

6. Bond forces between concrete and steel appear small in all the steel elements. The existence of perfect bond between steel and concrete in the elastic range seems justifiable.

4.3.2.2 CRACK INITIATION AND PROPAGATION

1. One primary crack is formed in the element 81 inside

the constant moment zone at a load of 580 lb. The principal tensile stresses in the concrete elements next to the steel elements in the constant moment zone approach the modulus of rupture.

2. The crack propagates upward with the increase of applied load and at a load level of 780 lb. additional cracks appear in the adjacent elements.

3. As additional concrete elements crack, the tensile stresses previously carried by these elements are now transferred to steel and a significant increase of steel stresses are noted. The increase is almost 90 % at a load level of 780 lb. as compared to the values at the initial load level.

4. As the crack propagates towards the compression zone, the principal tensile stresses of the concrete elements at the tip of the cracks decrease.

5. The strains in the uncracked concrete elements trapped in between cracked elements decrease compared to the values they achieved at the elastic stage.

6. The shear stresses in the concrete increase as the load increases and with the crack propagating upwards. At 780lb. theconcrete shear stresses increase by 24 % in the uncracked zone with respect to the values corresponding to

the initial load. he remaining shear stresses carried by the cracked elements are very small.

7. Approximately 3% of the shear is carried by steel in the elastic range. The figure rises upto 12 % when cracks begin forming.

CHAPTER 5

SUMMARY AND CONCLUSIONS

5.1 SUMMARY AND CONCLUSIONS

The present study deals with the nonlinear finite element analysis of two dimensional reinforced concrete members under monotonically increasing loads. The analysis of the reinforced concrete members considered the sources of nonlinearity such as stress-strain relationship, cracking of concrete, post cracking behavior, reactions at the interface of concrete and steel and the yielding of reinforcement.

A simply supported singly reinforced concrete beam and a simply supported doubly reinforced concrete beam were analysed. The deflections of the entire nodes at all the load levels and the corresponding bond stress - bond slip values were part of the computer output obtained .

Spokowski's model eliminates the cracked concrete elements. The presented program incorporates the residual strength of the cracked concrete parallel to the crack. The results suggest a tendency for increased yield and failure loads of the cracked model.

The cracking pattern obtained agrees well with the logical reasoning . Especially all the concrete cover elements in the constant moment zone cracked at the same load level.

The load deflections show good agreement initially with the experimental values. But towards the ultimate stages it shows differences.

From the above analysis it seems that if a phenomenon affecting the behaviour of the reinforced concrete member is known it can be modelled quite easily.With an adequately refined finite element technique, all the specific properties and behaviours can be modelled and any reinforced concrete member can be analysed effectively.

5.2 SUGGESTIONS FOR FUTURE RESEARCH

The refinement and improvement of a finite element model has to be approached in two different levels simultaneously. One level is to improve the efficiency of the program through the employment of modern efficient equation solvers, powerful iterative methods suited to the type of analysis desired. The other one is the improved understanding of the material behaviors.

More experimental work is required on the crack formation and propagation. A crack is usually defined by the tensile strength of the concrete element and it would be desirable to determine an exact direction of propagation irrespective of the finite element mesh utilysed.

Incorporation of a complete and general stress-strain

behaviour model with cyclic loadings which covers all biaxial and triaxial stress-strain fields is highly desirable.

More experimental data on the crack width and the relative displacement parallel to the cracks at different load levels is required. This will enable development of a more accurate model to represent both the aggregate interlock mechanism and dowel action phenomenon to be used in the nonlinear finite element analysis of two dimensional concrete structures.

A simple analytical model which accounts for gradual release of tensile stresses after cracking is desirable than the sudden release of concrete tensile stresses upon cracking. More experimental work is required in determining a value for the ultimate strain at which complete release of the tensile stresses in cracked concrete takes place. This would then allow for simple expressions to be developed for the gradual release of tensile stresses of concrete.

The contribution of post cracking shear resistance must be included rather than neglecting its effects in the analysis.

Also the simulation of time dependent charecteristics of concrete such as creep and shrinkage is important. However, the choice of the most general and best failure criterion for the concrete, suited to the specific kind of problem will always be essential.

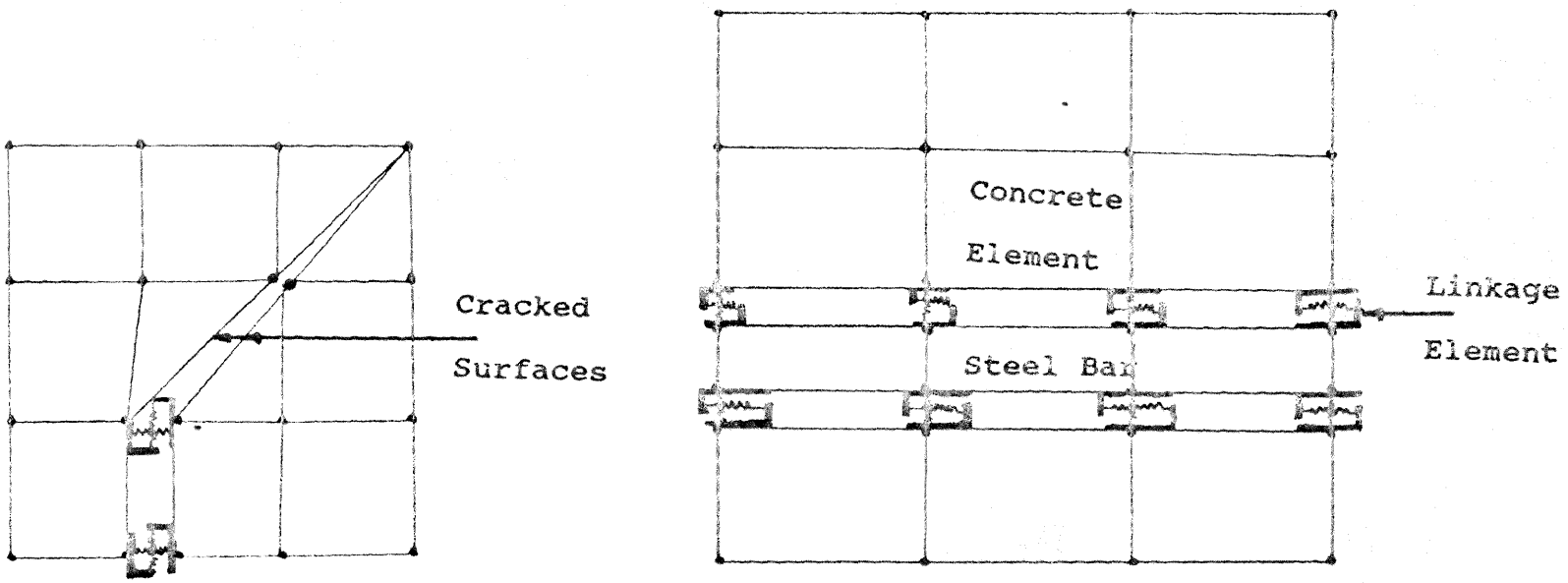

FIG.1 LINKAGE ELEMENTS USED IN DISCRETE CRACKING MODEL

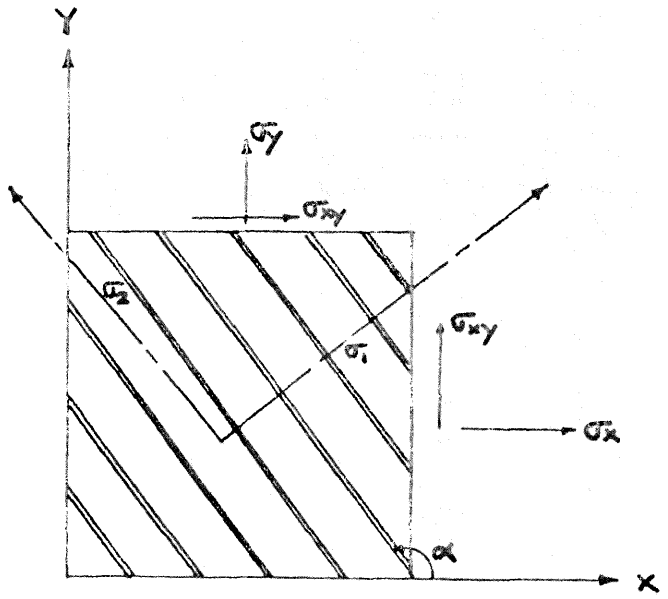

FIG.2. SMEARED CRACKING REPRESENTATION

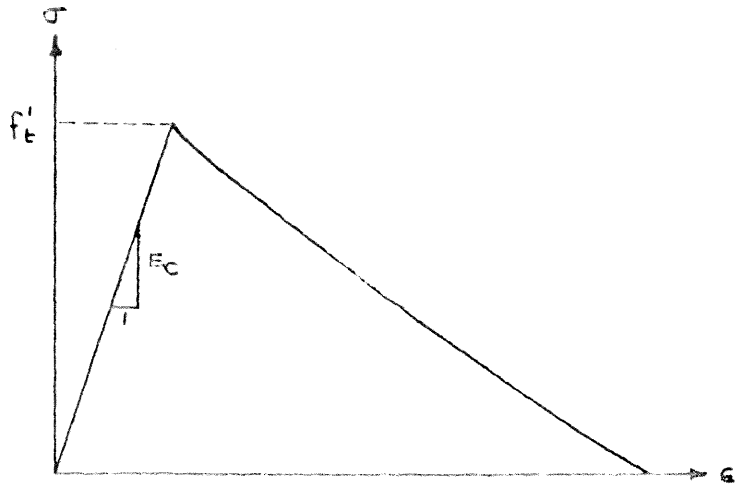

a . Stress-Strain Curve for Concrete in Tension

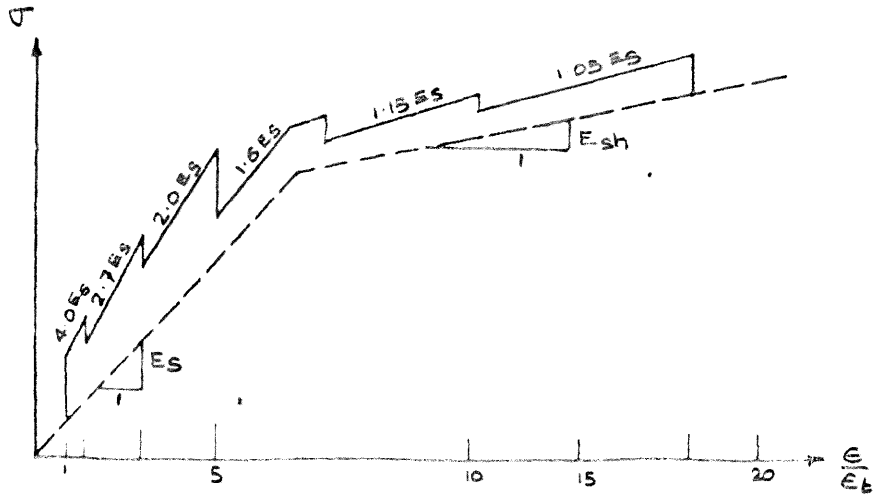

b. Modified stress-Strain Curve for Reinforcing Steel(40)

FIG.3. MODELS TO ACCOUNT FOR TENSION STIFFENING IN CONCRETE AFTER CRACKING

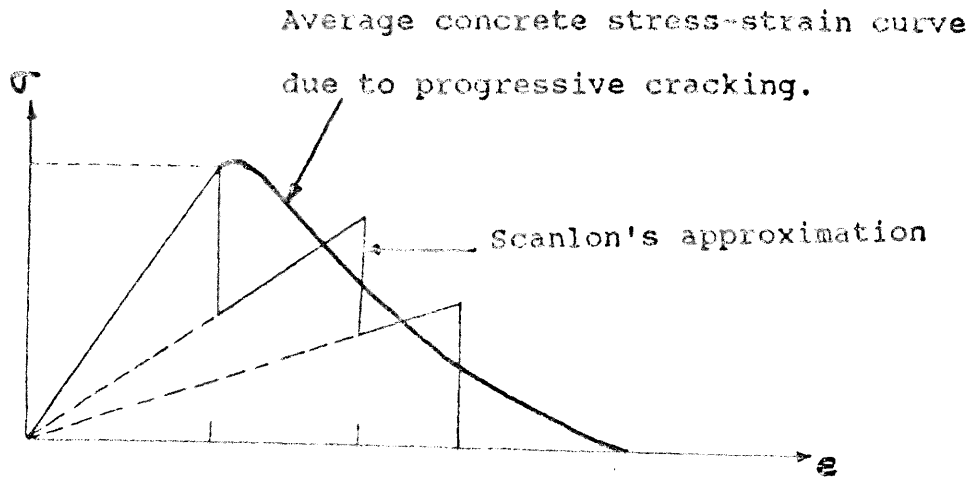

FIG. 4 SCANLON'S STEPPED MODEL (39)

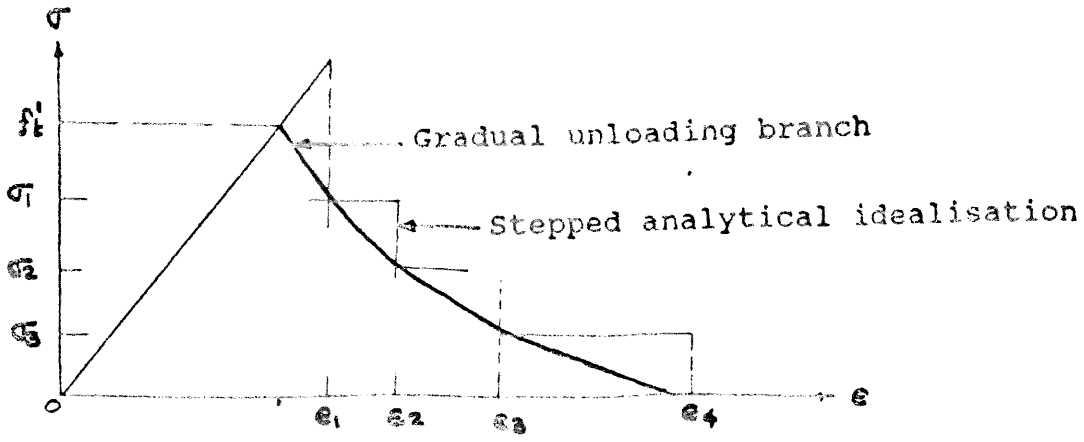

FIG. 5. LIN'S GRADUALLY UNLOADING MODEL (37)

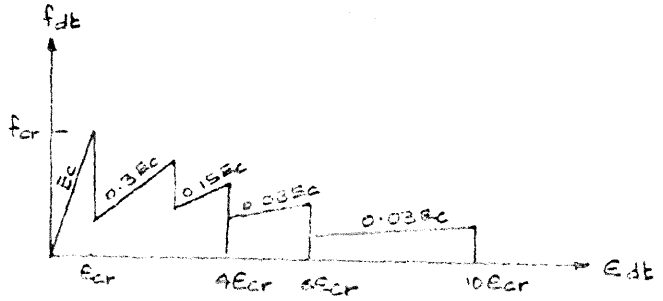

a. STEPPED RESPONSE AFTER CRACKING

b. GRADUAL UNLOADING RESPONSE AFTER CRACKING

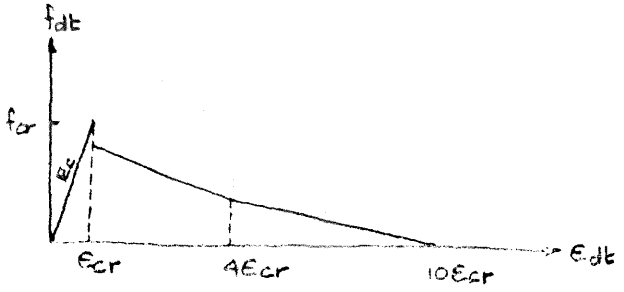

c. DISCONTINUOUS RESPONSE AFTER CRACKING

FIG.6. STRESS-STRAIN CURVES FOR CONCRETE IN TENSION (38)

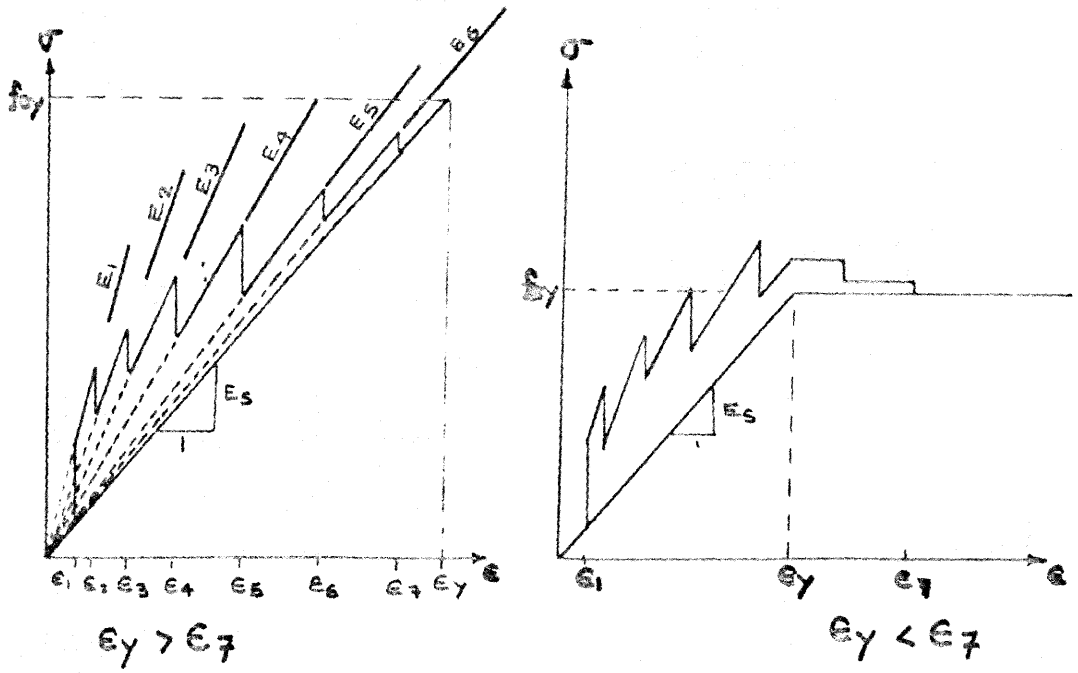

Material Modelling Law

ϵ_1	ϵ_2	ϵ_3	ϵ_4	ϵ_5	ϵ_6	ϵ_7
ϵ_{cr}	$1.5\epsilon_{cr}$	$3\epsilon_{cr}$	$5\epsilon_{cr}$	$8\epsilon_{cr}$	$11\epsilon_{cr}$	$14\epsilon_{cr}$

E_1	E_2	E_3	E_4	E_5	E_6
$4.0E_s$	$2.7E_s$	$2.0E_s$	$1.6E_s$	$1.15E_s$	$1.05E_s$

FIG.7. MODIFIED STRESS-STRAIN DIAGRAMS FOR TENSION STEEL AFTER CRACKING (38)

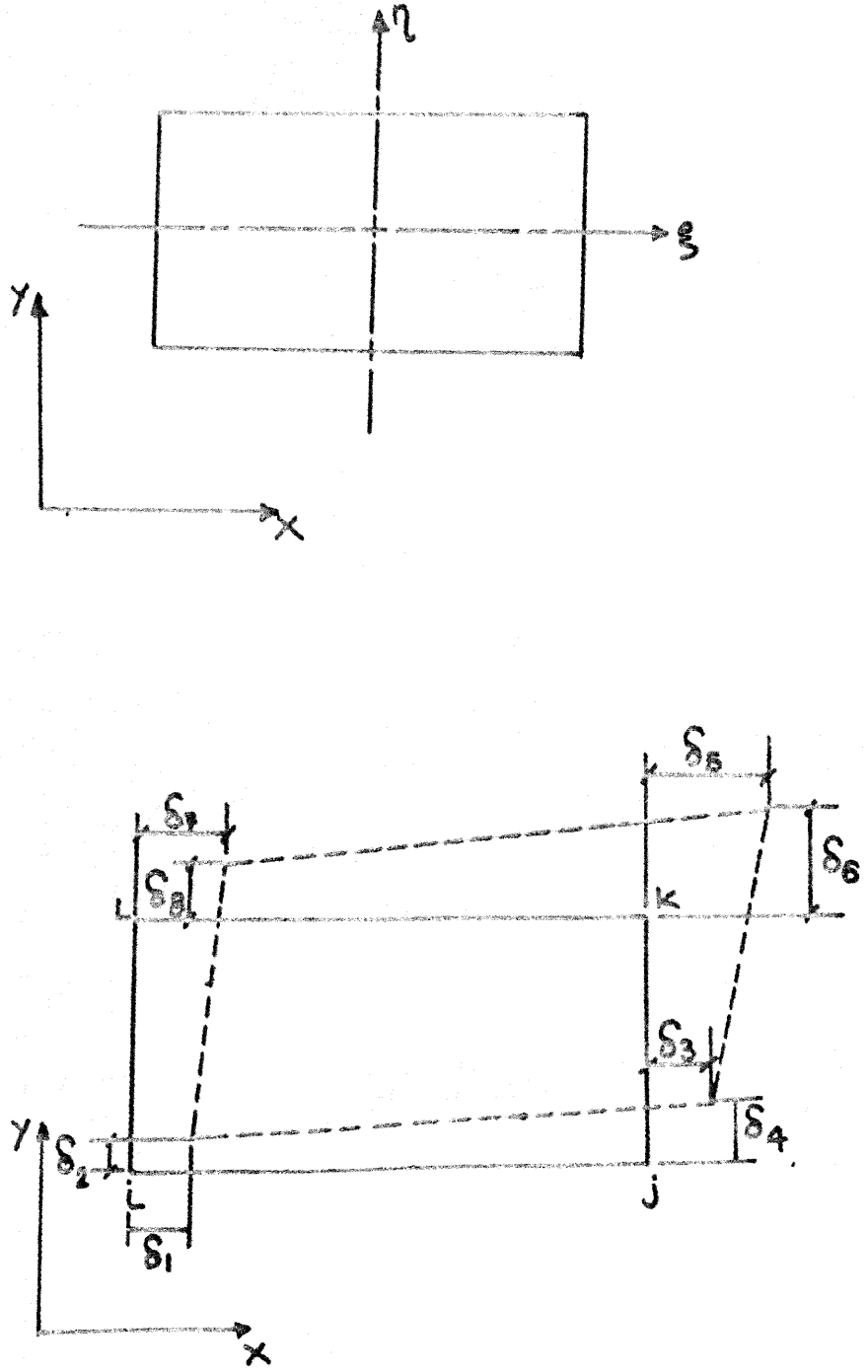

FIG.8. RECTANGULAR 4 NODE ELEMENT AND END DISPLACEMENTS.

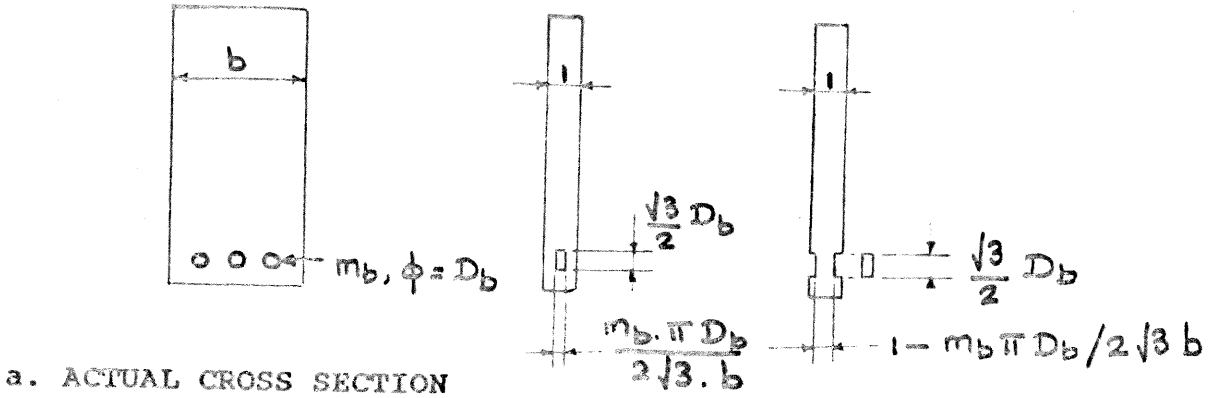

a. ACTUAL CROSS SECTION

b. UNIT TRANSFORMED CROSS SECTION

FIG. 9. REPRESENTATION OF REINFORCED CONCRETE CROSS SECTION

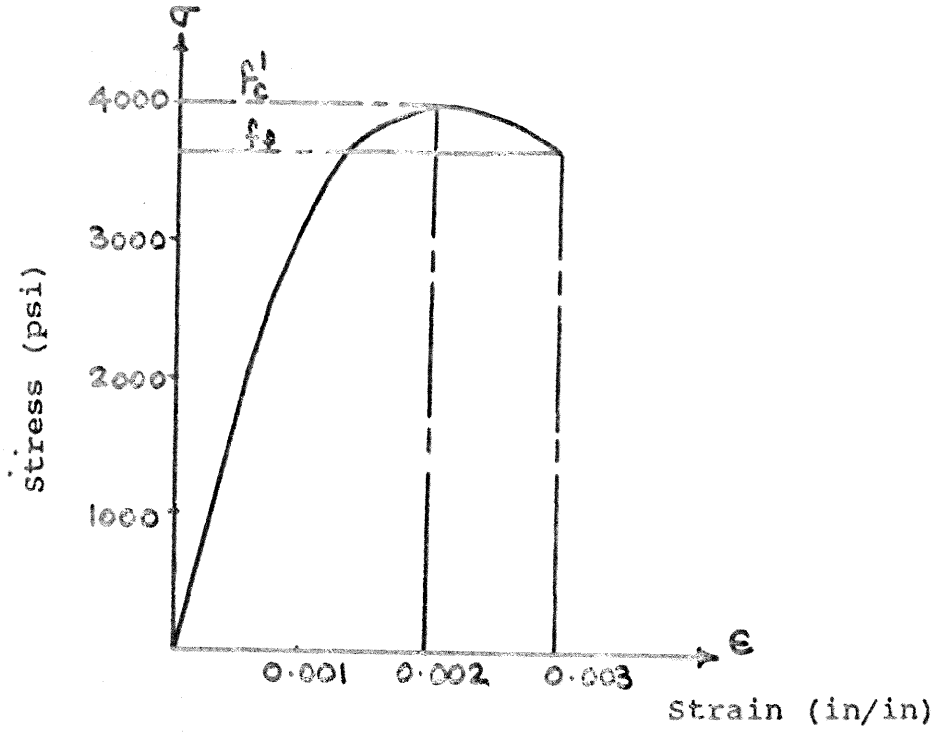

FIG.10. CONCRETE STRESS-STRAIN CURVE BY SAENZ FOR 4000 PSI CONCRETE

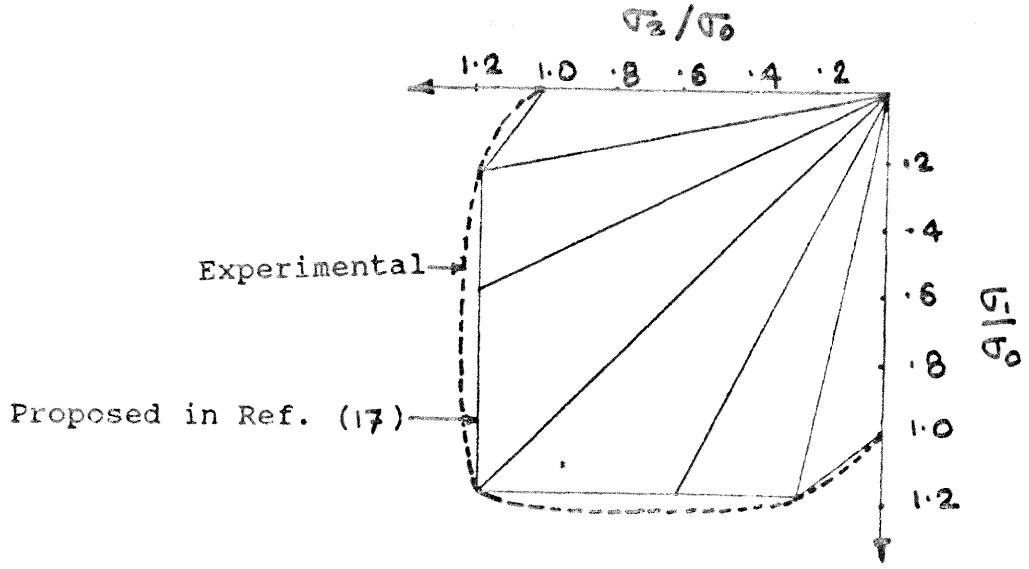

FIG.11. FAILURE ENVELOPE FOR CONCRETE UNDER BIAXIAL COMPRESSION

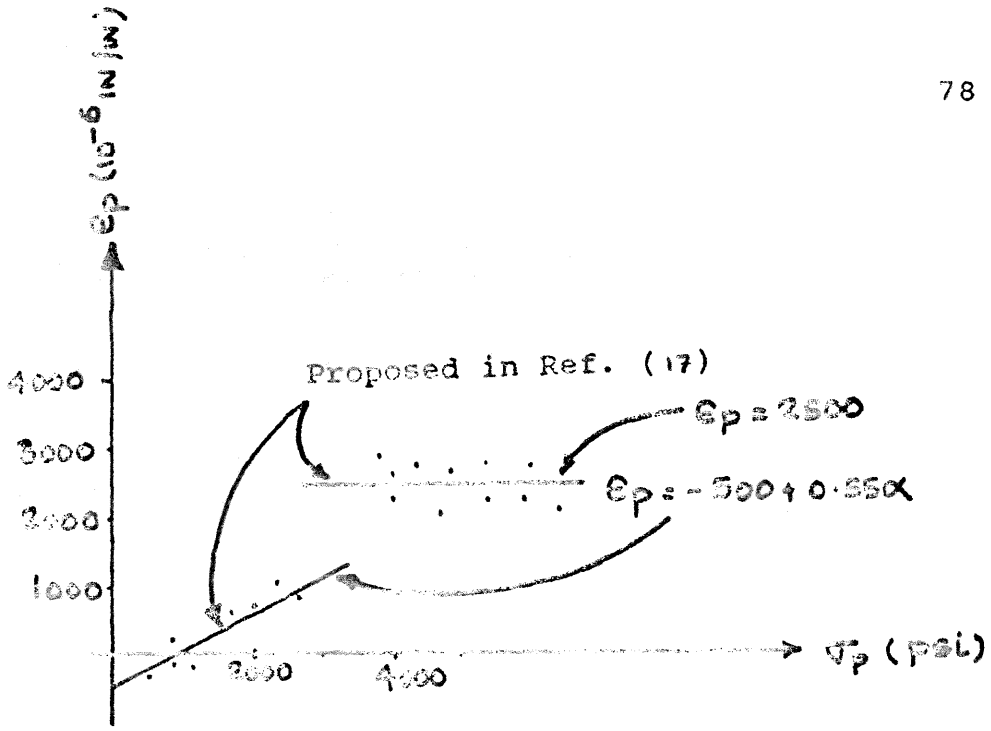

FIG.12. ULTIMATE STRAIN VS ULTIMATE STRESS FOR CONCRETE UNDER BIAXIAL COMPRESSION

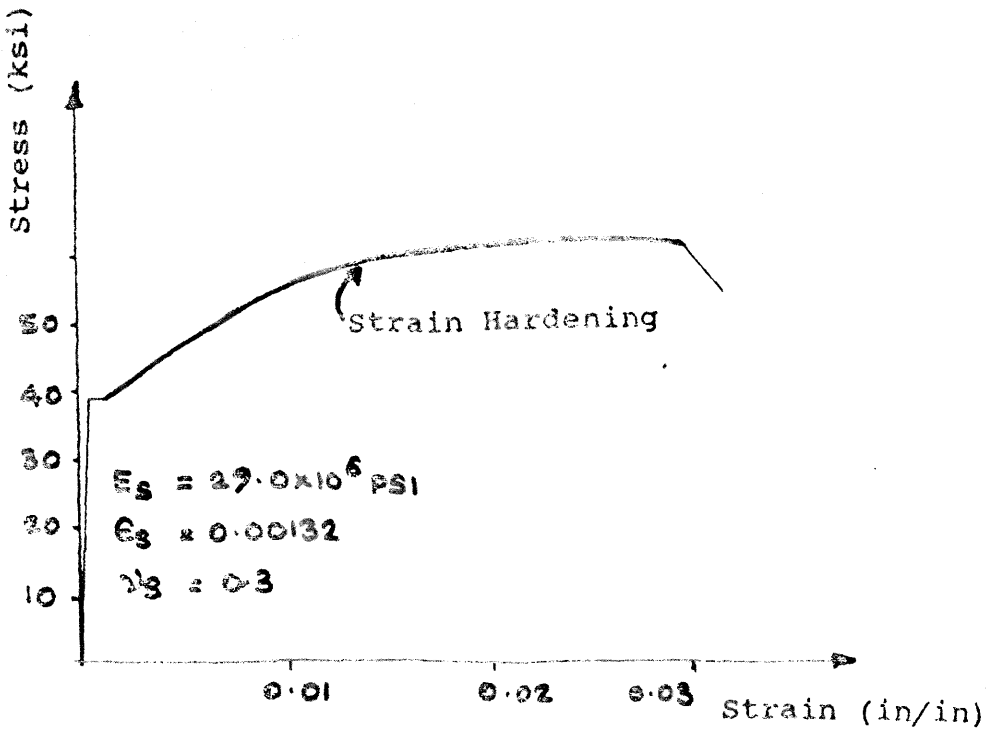

FIG.13. STEEL STRESS-STRAIN CURVE

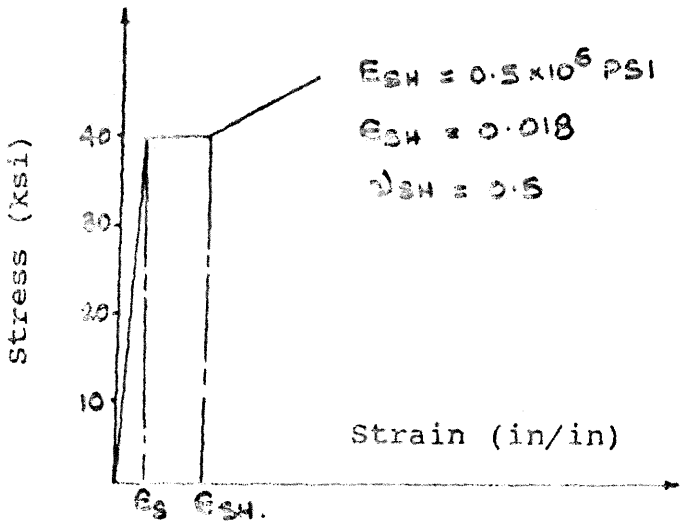

FIG.14. MODIFIED STEEL STRESS-STRAIN CURVE

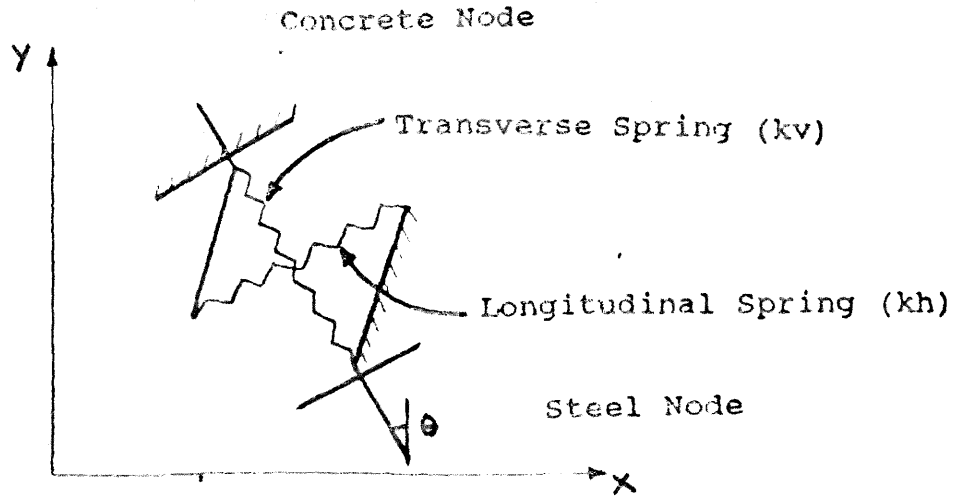

FIG.15. CONCEPT OF LINKAGE ELEMENT

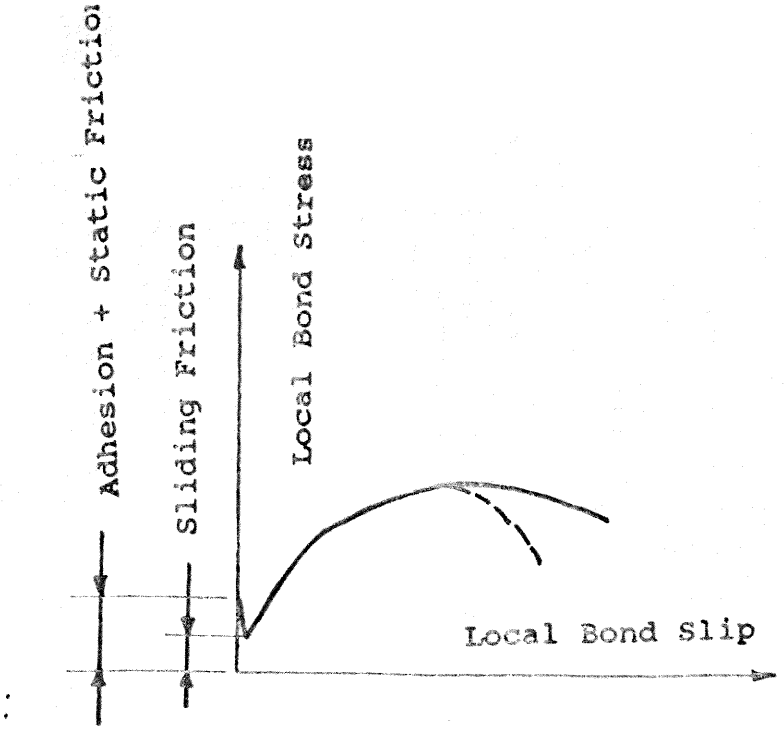

FIG.16. BOND STRESS-SLIP CURVES

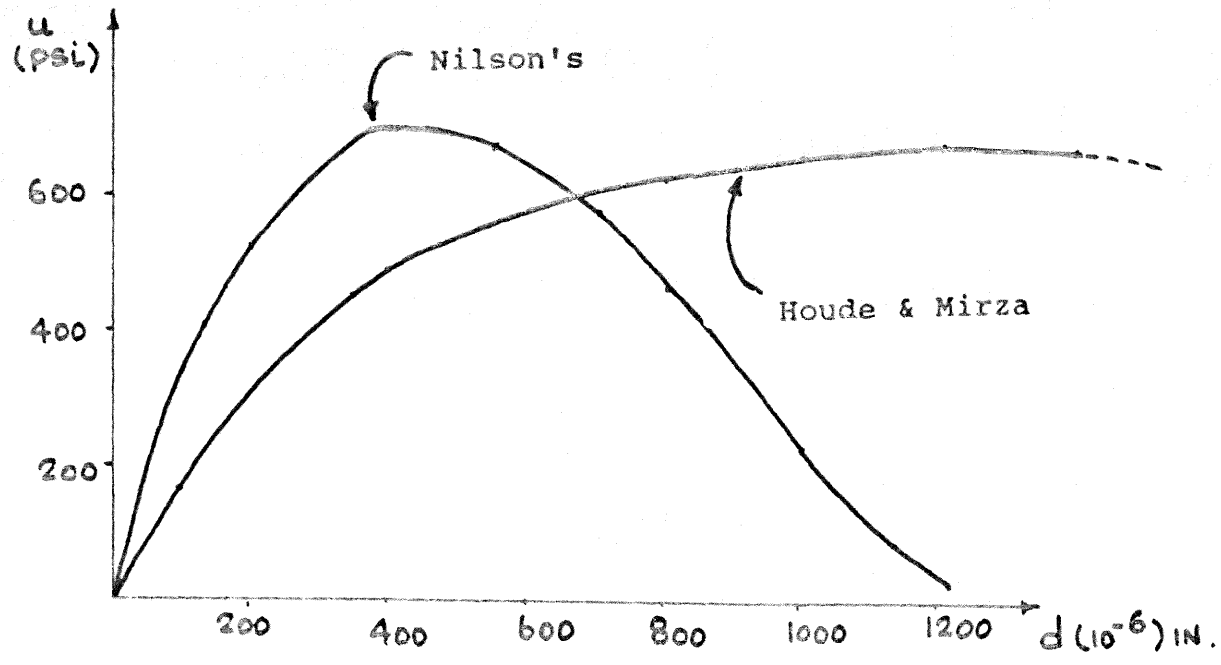

FIG.17. BOND STRESS-SLIP CURVES

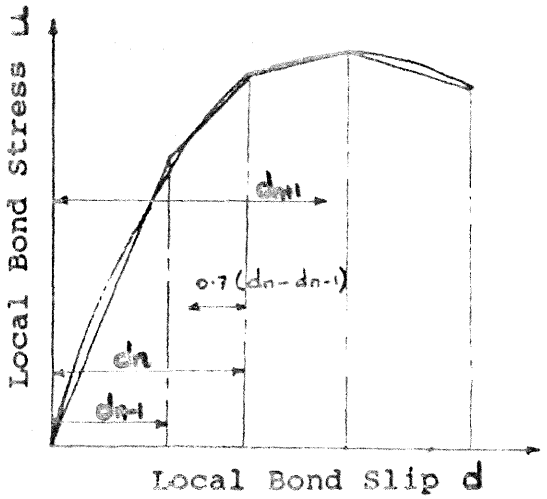

FIG.18. PREDICTED BOND SLIP FOR LOADING STEP N+1

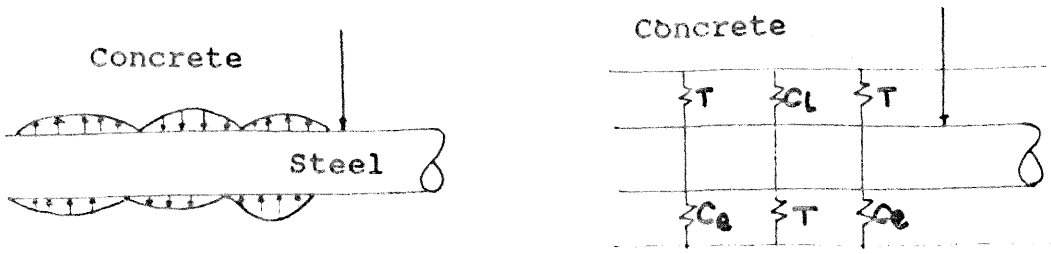

FIG.19. COMPRESSIVE AND TENSILE SPRINGS

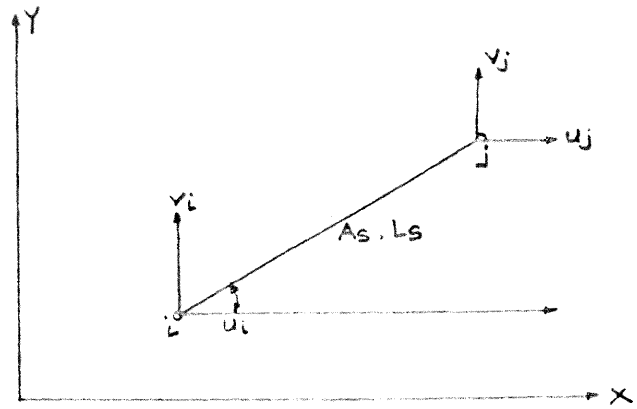

FIG.20. STIRRUP BAR ELEMENT

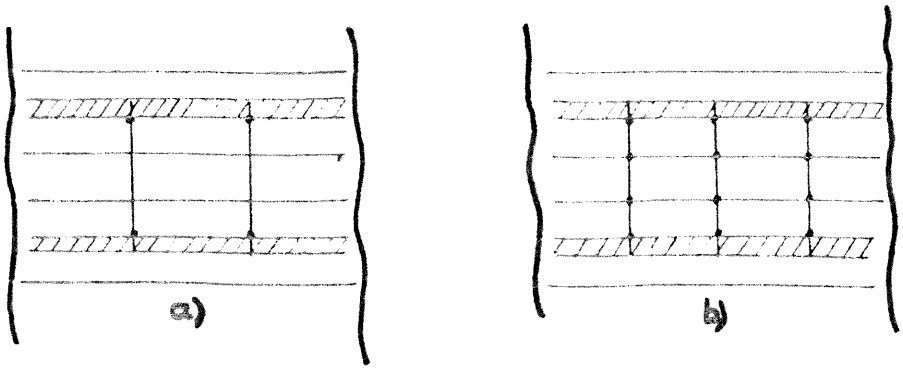

FIG.21. DIFFERENT MODELLING OF STIRRUP

8	16	24	32	40	48	56	64	72	80	88
7	15	23	31	39	47	55	63	71	79	87
6	14	22	30	38	46	54	62	70	78	86
5	13	21	29	37	45	53	61	69	77	85
4	12	20	28	36	44	52	60	68	76	84
2	10	18	26	34	42	50	58	66	74	82
1	9	17	25	33	41	49	57	65	73	81

CONCRETE ELEMENTS

3	11	19	27	35	43	51	59	67	75	83

STEEL ELEMENTS

FIG.22. CONCRETE AND STEEL ELEMENT OF TEST BEAM 1.

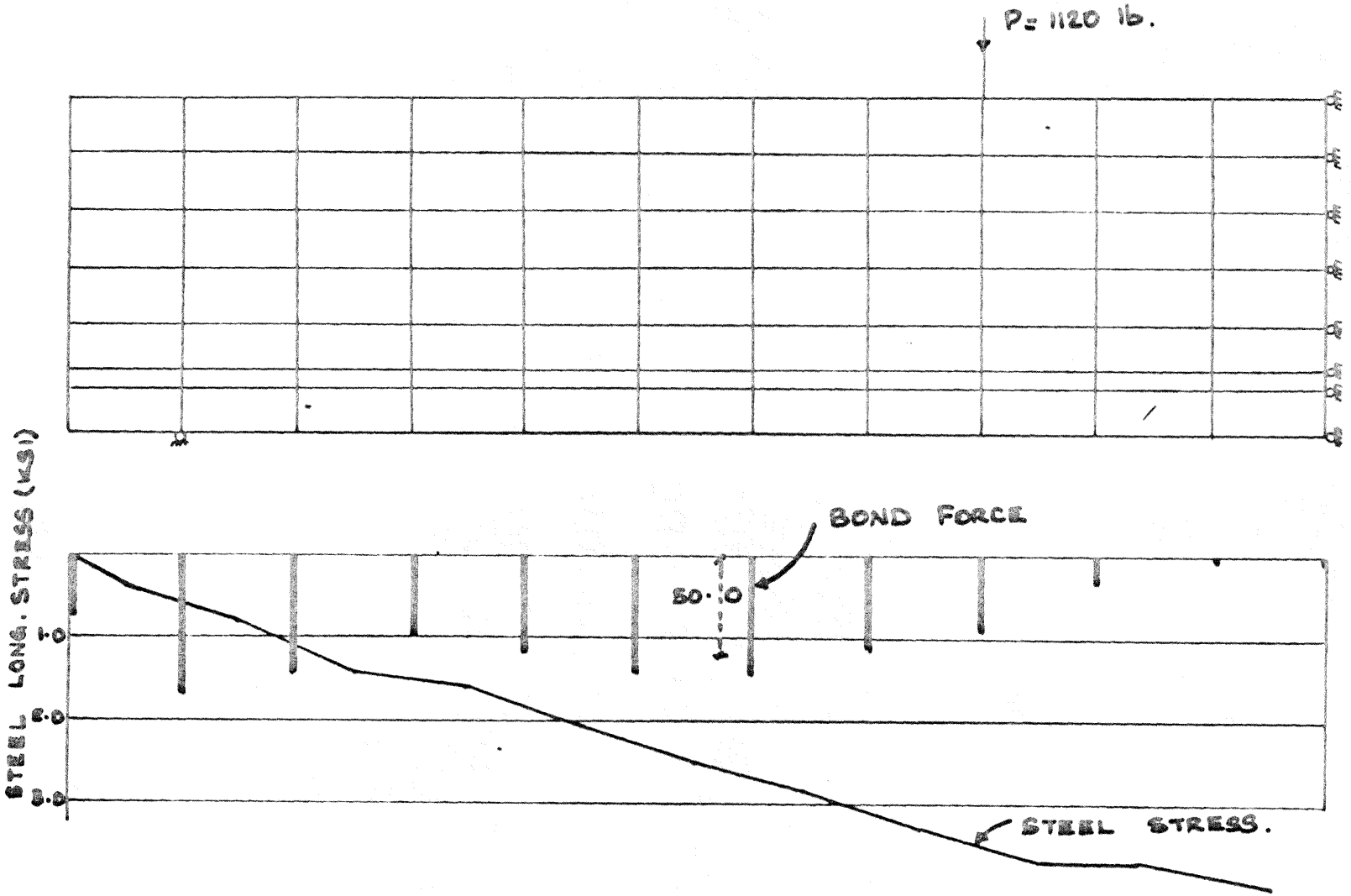

FIG.23. STRESS AND BOND FORCE DISTRIBUTIONS OF TEST BEAM 1

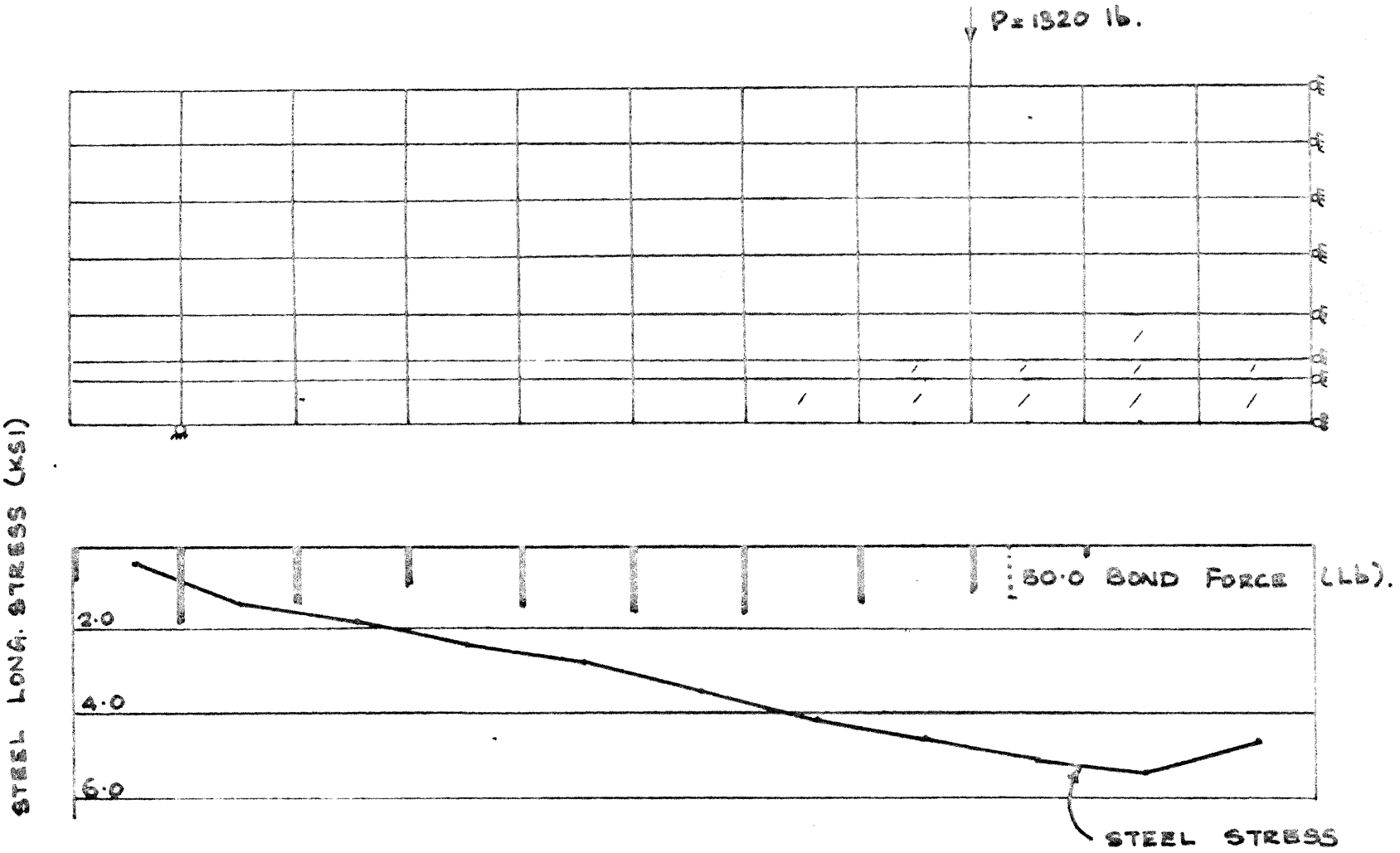

FIG.24. . STRESS AND BOND FORCE DISTRIBUTIONS OF TEST BEAM

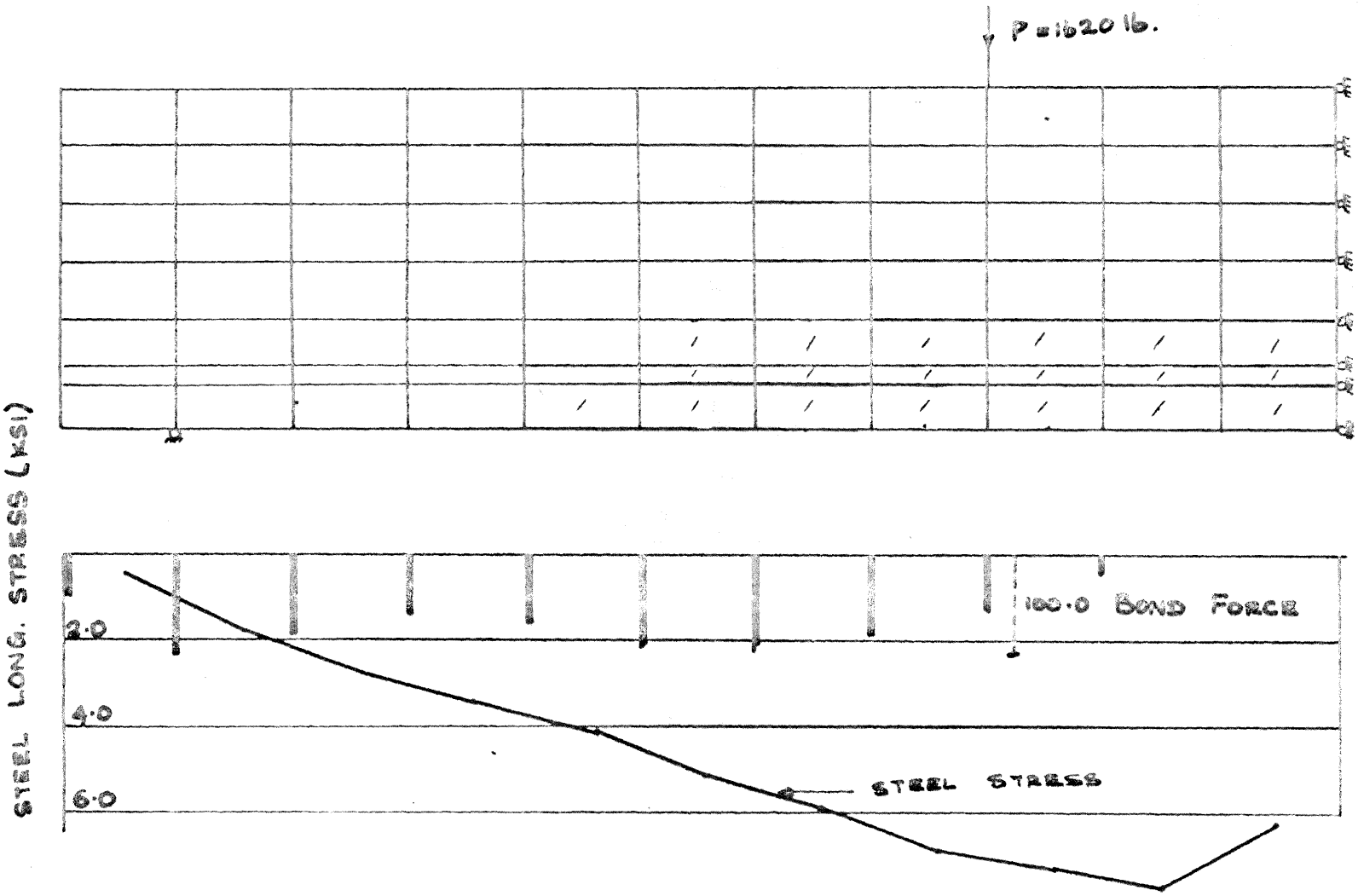

FIG.25. STRESS AND BOND FORCE DISTRIBUTIONS OF TEST BEAM

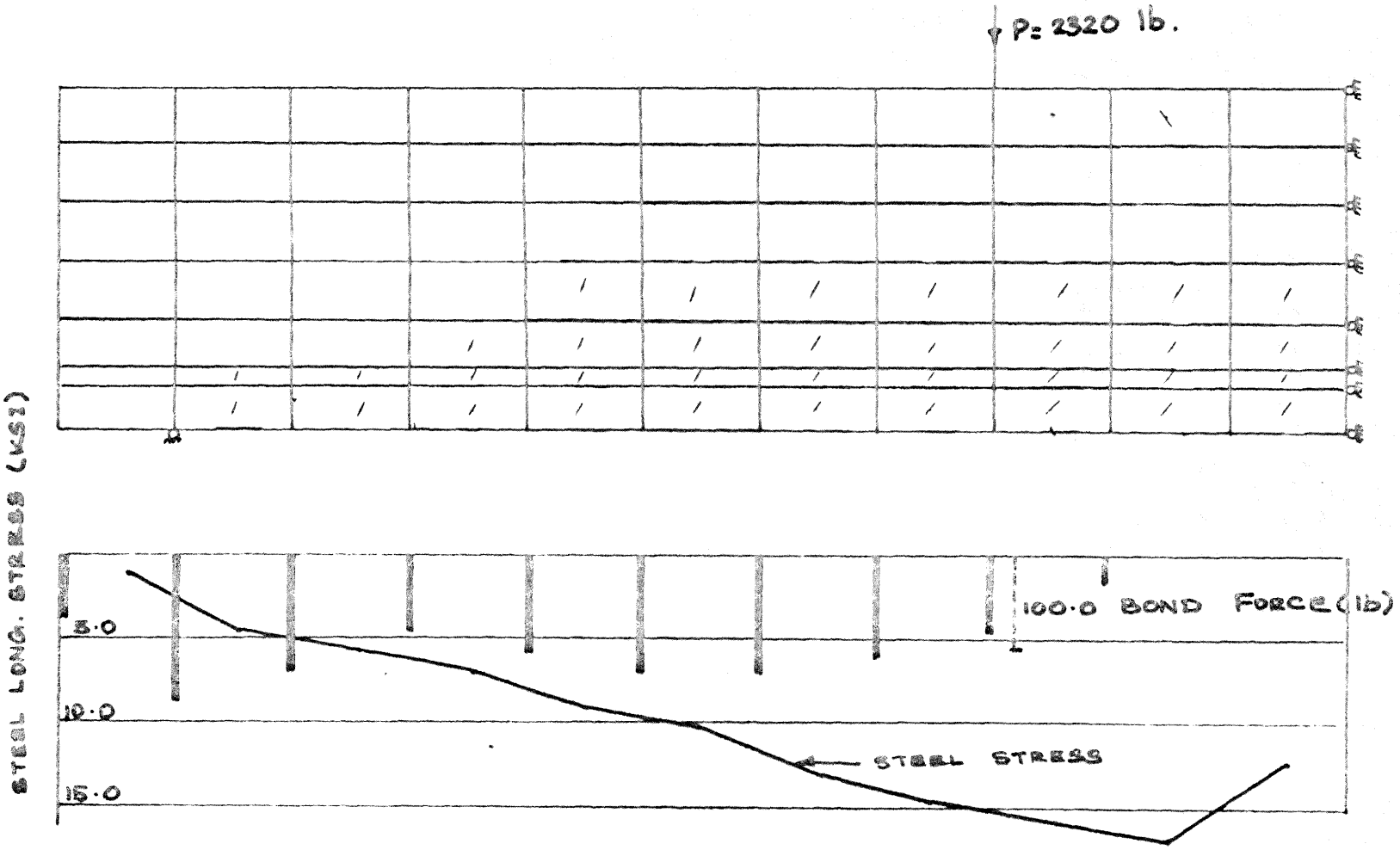

FIG.26. STRESS AND BOND FORCE DISTRIBUTIONS OF TEST BEAM 1.

9	19	29	39	49	59	69	79	89	99

STEEL ELEMENTS OF TOP R/F

10	20	30	40	50	60	70	80	90	100
8	18	28	38	48	58	68	78	88	98
7	17	27	37	47	57	67	77	87	97
6	16	26	36	46	56	66	76	86	96
5	15	25	85	45	55	65	75	85	95
4	14	24	34	44	54	64	74	84	94
2	12	22	32	42	52	62	72	82	92
1	11	21	81	41	51	61	71	81	91

CONCRETE ELEMENTS

3	13	23	33	43	53	63	73	83	93

STEEL ELEMENTS OF BOTTOM R/F

FIG.27. CONCRETE AND STEEL ELEMENTS OF TEST BEAM 2.

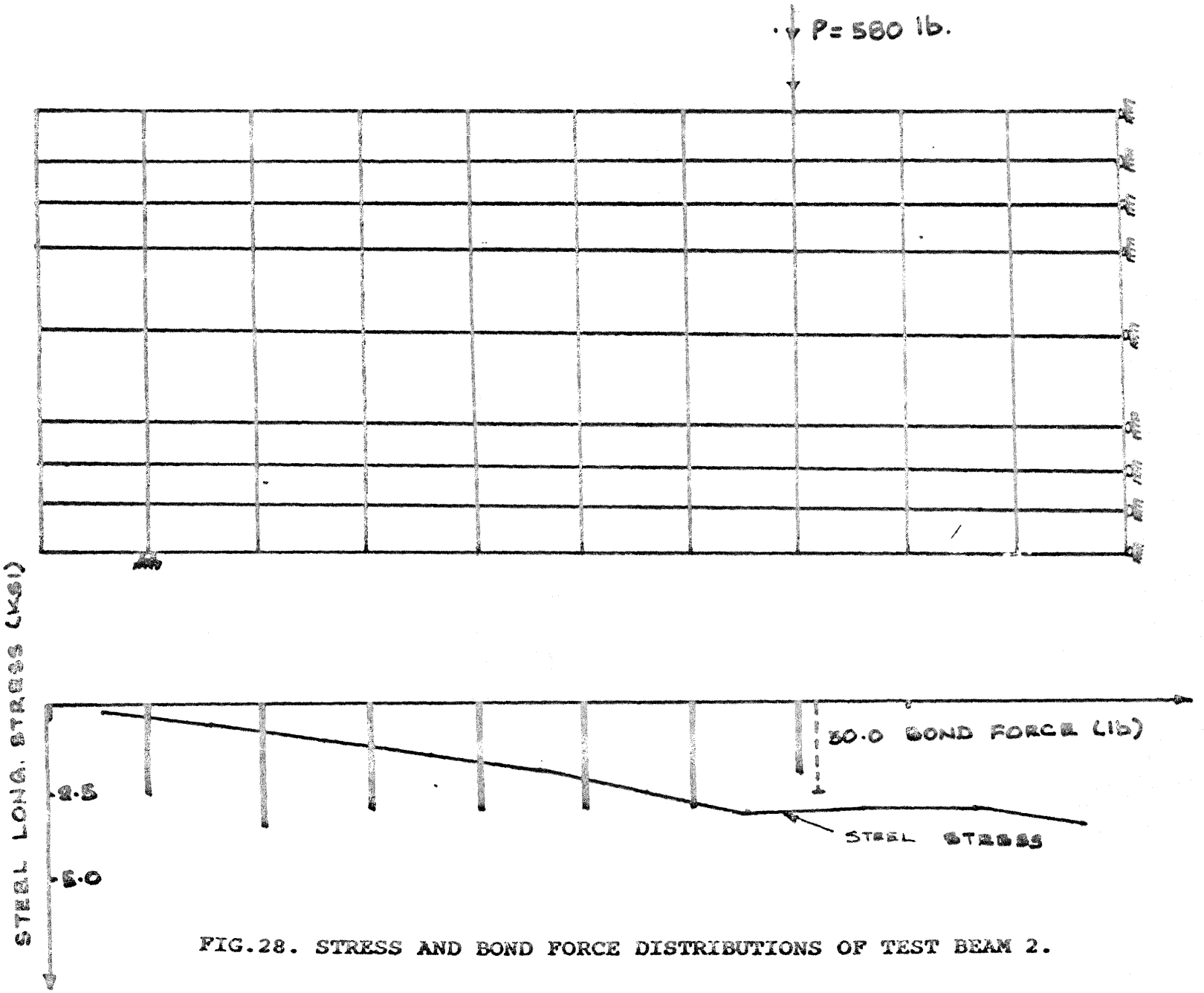

FIG.28. STRESS AND BOND FORCE DISTRIBUTIONS OF TEST BEAM 2.

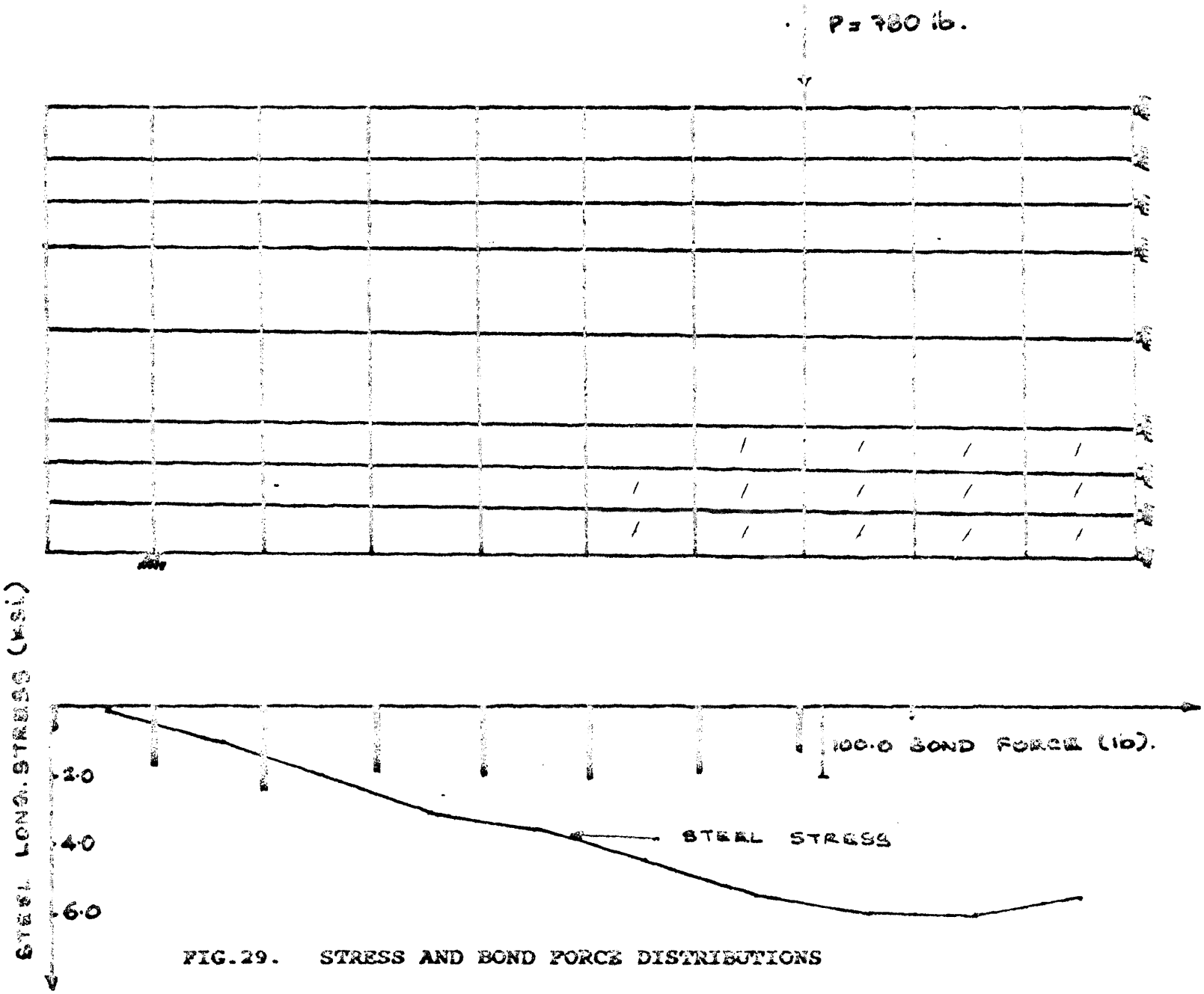

FIG. 29. STRESS AND BOND FORCE DISTRIBUTIONS OF TEST BEAM 2.

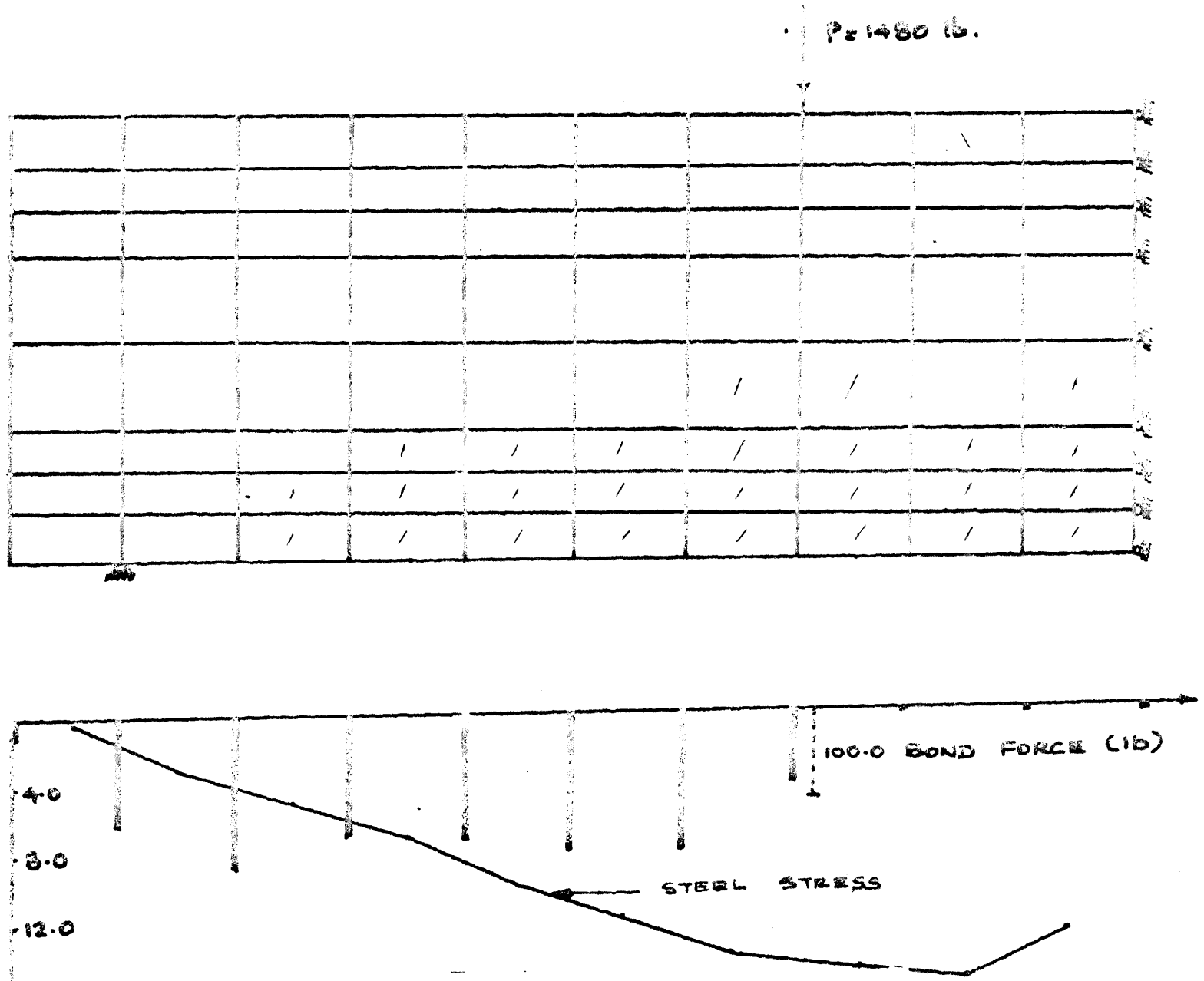

FIG.30. STRESS AND BOND FORCE DISTRIBUTION OF TEST BEAM 2.

REFERENCES

1 . ACI Standard 318 , Building Code Requirements for Reinforced Concrete , American Concrete Institute , 1977.

2 . Canadian Standards Association , "Code for the Design of Concrete Structures for Buildings , Can-A23-3-M77" , Canadian Standards Association, Rexdale, Ontario, 1977.

3 . Ngo, D., and Scordelis, A.C., "Finite element analysis of reinforced concrete beams", Journal ACI, Vol. 64, No. 3, March 1967, pp. 152-163.

4 . Nilson, A.H., "Nonlinear analysis of reinforced concrete by the finite element method", ACI Journal, Vol. 65, No. 65-9, Sept. 1968.

5 . Saenz, L.P., Discussion of "Equation for the Stress-Strain curve of concrete", by P.Desai and S.Krishnan, ACI Journal, Vol. 61, Sept.1964, pp. 1229-1235.

6 . Nilson, A.H., "Nonlinear analysis of reinforced concrete by the finite element method", ACI Journal, vol. 69 no. 7, july 1972, pp. 439-441.

7 . Franklin, H.A., "Nonlinear analysis of reinforced concrete frames and panels", Ph.D. Thesis, University of California, Berkely, California, March, 1970.

8 . Cervenka, V. and Gerstle, K.H., "Inelastic finite element analysis of reinforced concrete panels under in-plane loads", Ph.D. Dissertation, University of Colorado, Boulder, Colorado, 1970.

9 . Yuzugullu.C and Schnobrich.W.C, "A numerical procedure for the determination of the behaviour of a shear wall frame system", ACI Journal, vol.7, july 1973, pp. 474-479.

10. Cedolin.L and Depoli .S , "Finite element non-linear plane stress analysis of reinforced concrete ", Construzioni in cemento armato, studi e rendicoti, vol. 13, 1976.

11. Bresler.B. and Scordelis.A.C , " Shear strength of reinforced concrete beams" , ACI Journal, vol.60, jan.1963, pp. 51-74.

12. Liu.C.Y, Nilson.A.H and Slate.F.O , "Biaxial stress-strain relationship for concrete", journal of the structural division, ASCE, vol.98, no.515, may 1972, pp. 1025-1034.

13. Darwin.D and Pecknold.D.A.W, " Inelastic model for cyclic biaxial loading of reinforced concrete" Civil Engineering Studies, STS no.409, University of Illinois, Urbana, Illinois, july 1974.

14. Agrawal A.B. Jaeger L.G and Mufti A.A, "Crack propagation and plasticity of reinforced concrete shear-wall under

monotonic and cyclic loading", in conference on finite element methods in engineering 1976, University of Adelaide, Adelaide, Australia, december 1976.

15. Al-Mahaidi, Riadh , S.H and Nilson.A.H " Nonlinear finite element analysis of reinforced concrete deep members" , research report no. 79-1, department of structural engineering , Cornel University, Ithaca, New York , 14853, jan. 1979, pp.374.

16. Tasuji.M.E. Nilson.A.H and Slate.F.O, "The behaviour of plain concrete subject to biaxial stress" report no. 360, dept. of structural engineering, Cornell University, Ithaca, New York, march 1976.

17. Spokowski.R.W "Finite element analysis of reinforced concrete members", M.Eng. thesis, structural concrete series no. 72-2,McGill University, Montreal, may 1972.

18. Houde.J "Study of the force-displacement relationship for the finite element analysis of reinforced concrete", Ph.D. Thesis, dept. of civil engineering and applied mechanichs, McGill University, Montreal , Oct. 1973.

19. Khouzam.M " A finite element investigation of reinforced concrete beams" M.Eng. thesis, McGill University, Montreal, oct. 1976.

20. Tokes.S.I. "Nonlinear finite element analysis of reinforced concrete members", M.Eng. thesis , McGill University, Montreal, august 1977.

21. Committee on finite element analysis of reinforced concrete structures, "State of the art report on finite element analysis of reinforced concrete", American society of civil engineers,N.Y, N.Y, 1982, pp.545.

22. Rashid.Y.R " Analysis of prestressed concrete pressure vessels", Nuclear engineering and design, vol.7 ,no.4, april 1980 pp. 334-355.

23. Kupfer.H.B and Gerstle.K.H " Behaviour of concrete under biaxial stresses" , journal of the engineering mechanichs division, ASCE, vol.99, no.EM4, proc. paper 9917, pp.852-866.

24. Romstad.K.M, Taylor.M.A and Herman.L.R, " Numerical biaxial characterisation for concrete", journal of the engineering mechanichs division,ASCE, vol.100, no.EMS, oct.1974, pp.935-948.

25. Gerstle.K.H, "Simple formulation of biaxial concrete behaviour", journal of the american concrete institute, vol.78,no.1, 1981, pp.62-68.

26. Liu .T.C.Y , Nilson A.H and Slate F.O, " Stress-strain response and fracture of concrete in uniaxial and biaxial

compression", journal of the american concrete institute, vol.68, no.5, may 1972, pp. 291-295.

27. Bazant.Z.P and Tsubaki.T, " Total strain theory and path dependence of concrete", journal of the engineering mechanichs division, ASCE, vol.106, No.EM, proc. paper 15911, dec.1980, pp.1151-1173.

28. Elwi.A.A and Murray.D.W , " A 3D hypoelastic concrete constitutive relationship", journal of the engineering mechanichs division, ASCE, vol.105, no. EM4, proc. paper 14746,aug.1979,pp. 623-641.

29. William.K.J and Warnke.E.P, " Constitutive model for the triaxial behaviour of concrete" , international association of bridge and structural engineers, seminar on concrete structures subjected to triaxial stresses, paper III-1, Bergamo, Italy, may 1974.

30. Chen.A.C.T and Chen.W.F, "Constitutive relations for concrete", journal of the engineering mechanichs division, ASCE, vol.101,No.EM4, aug.1975,pp. 465-481.

31. Bazant.Z.P and Kim.S.S, "Plastic-fracturing theory for concrete", journal of the engineering mechanichs division, proceedings, ASCE, vol.105, june 1979, pp. 407-428.

32. Saouma.V , " Automated nonlinear finite element analysis

of reinforced concrete: A fracture mechanichs approach", Ph.D. thesis, Cornell University ,N.y ,jan.1981.

33. Hand, F.R, Pecknold.D.A and Schnobrich.W.C, " Nonlinear layered analysis of r/c plates and shells", journal of the structural division , ASCE, vol.99, no.ST7, july 1973, pp. 1491-1505

34. Agrawal.A.B, " Nonlinear analysis of reinforced concrete planar structures subject to monotonic, reversed cyclic and dynamic loads", Ph.D. thesis, University of New Brunswick, Fredriction, N.B, march 1977.

35. Cedolin.L and Dei Poli.S , " Finite element studies of shear critical reinforced concrete beams", journal of the engineering mechanichs division, ASCE, vol.103, june 1977, pp. 395-410.

36. Paulay.T and Loeber.P.S , " Shear transfer by aggregate interlock", shear in reinforced concrete, vol.1, special publication sp-42, ACI, Detroit, Michigan 1974.

37. Lin.C.S and Scordelis.A , " Nonlinear analysis of r/c shells of general form", journal of the structural division,ASCE, proc. paper 11164, march 1975 pp. 523-538.

38. Gilbert.R.I and Warner.R.I, " Tension stiffening in r/c slabs", journal of the structural division, ASCE, vol.104,

dec. 1978, pp. 1885-1900.

39. Scanlon.A, " Time dependent deflections of reinforced concrete slabs", Ph.D. thesis , University of Alberta, Edmonton, Alberta, 1971.

40. Van Grunen.T, " Nonlinear geometric , material and time dependent analysis of reinforced and prestressed concrete slabs and panels", UC-SESM report no. 79-3,University of California, Berkely , oct.1979. pp.275.

41. Mylrea.T.D, " Bond and anchorage", ACI journal , proceedings, vol.44, march 1948.

42. Lutz.L.A Gergely.P and Winter.G , " The mechanichs of bond and slip of deformed reinforcing bars in concrete", structural engineering report no. 234, Cornell University, N.Y, aug. 1966.

43. Broms.B.B, " Technique for investigation of internal cracks in reinforced concrete members", ACI journal, vol.62, jan.1965, pp. 35-44.

44. Goto.Y, " Cracks formed in concrete around deformed tension bars", ACI journal , vol.68, april 1971, pp. 244-251.

45. Mirza.M.S and Houde.J, " Study of bond stress-slip relationship in reinforced concrete", ACI journal, proceedings , vol.76, jan.1979, pp.19-46.

46. Turner.J.J, Clough.R.W, Martin.H.C, Topp.L.J, "Stiffness and deflection analysis of complex structures ". Journal of aeronautical sciences, vol.23, no.9, sept. 1956.

47. Zienkiewicz.O.C, " The finite element method in engineering science ", London, 1971, Mcgraw Hill.

48. Nilson.A.H, " Finite element analysis of reinforced concrete " , Ph. D. Dissertation, University of California, Berkeley, 1967.

49. Ngo.D, Scordelis.A.C, and Franklin.H.A, " Finite element study of reinforced concrete beams with diagonal tension cracks ", UCSESM report no. 70-19, University of California, Berkeley, 1970.

50. Mufti.A.A, Mirza.M.S, McCutcheon.J.O and Spokowski.R.W, " A study of non-linear behaviour of structural concrete elements" proceedings of the specialty conference on finite element method in civil engineering, McGill University, Montreal, june 1972.

51. Valliappan.S and Nath.P, " Tensile crack propagation in reinforced concrete beams - finite element technique " , International conference shear, torsion and bond in reinforced and prestressed concrete, Coimbatore, India, 1969.

52. Valliappan.S and Doolan.T.F, "Non-linear stress analysis

of reinforced concrete structure by finite element method", UNICIV report no. r-72, University of New South Wales, 1971.

53. Zienkiewicz.O.C, Valliappan.S and King.I.P, " Stress analysis of rock as a no tension material ", Geotechnique, vol.18, no.1, 1968.

54. Houde,J and Mirza.M.S, " A study of bond stress-strain relationships in reinforced concrete" , Structural concrete series no.72-8, McGill University, Montreal, April 1972.

55. Loov.R.E, " Finite element analysis of concrete members considering the effects of cracking and the inclusion of reinforcement ", Ph.D. Dissertation, University of Cambridge, Cambridge, 1970.

56. Hughes.B.P and Chapman.G.P, " Complete stress-strain curve for concrete in direct tension", RILEM Bulletin, no.30, march 1966.

57. Popovics.S, " Review of stress-strain relationships for concrete ", journal of the ACI, vol.67,no.3, 1970.

58. Newman.K, " Criteria for the behaviour of plain concrete under complex states of stress" , proceedings of an international conference on the structure of concrete and its behaviour under load, London,1965.

59. ACI committee 335 draft report " Deflection of concrete

beams", april 1963.

60. ACI committee 408, " Bond stress - State of the art ", journal of the ACI, vol.63, no.11, 1966.

61. Dulacska.H, " Dowel action of reinforcement crossing cracks in concrete", journal of the ACI, vol.69,no.12, 1972.

62. Bressler.B and Bertero.V, " Influence of load history on cracking of reinforced concrete", report to California division of highways, department of civil engineering, University of California, Berkeley, 1966.

63. Nilson.A.A, " Bond stress-slip relations in reinforced concrete", school of civil and environmental engineering, Cornell University, N.Y, report 345, december 1971.

64. Will.G.T, Uzumeri.S.M, Sinha.S.K, " Application of the finite element method to the analysis of reinforced concrete beam-column joints",proceedings of the specialty conference on finite element method in civil engineering, McGill University, Montreal, june 1972.

65. Kaplan.M.F, " The application of fracture mechanics to concrete", proceedings of an international coference on the structure of concrete and its behaviour under loads, London,1965.

66. Irwin.G.R, " Fracture mechanics", proceedings of the

first symposium on naval structural mechanics, New York, Pergamen Press, 1960.

APPENDIX : COMPUTER PROGRAM

A.1 DESCRIPTION

The computer program used is coded in Fortran IV, G.Level, and iscompatible with the O/S system of the I.B.M. 360/75 computer. In the given form it is capable of analysing plane structures with the following parameters:

350 nodes

250 quadrilateral elements

150 spring elements

30 nodal point boundaries

20 partitions

40 stirrups

350 nodes at which loads may be applied

45 nodes in a partition

The idealised structure should be partitioned to have a consecutive nodal numbering system. Only one partition line, not necessarilly a straight line, should pass through an element.

The datas should be reduced to a unit width of the member.

The numbering of the element is in the anti-clockwise direction.

The element nodal coordinates are input with respect to the

global X-Y axes.

The datas are submitted in the following sequence:

NOTATION	DESCRIPTION
	STRUCTURE PROPERTIES
NPART	Total number of partitions
NPOIN	Total number of nodal points
NELEM	Total number of elements
NBOUN	Total number of nodes with prescribed displacements
NCOLN	Total number of different loadings
NFREE	Number of degrees of freedom per node
NCONC	Total number of concentrated loads
NYM	Total number of different elastic properties
NS	Total number of stirrups
	NODAL POINT ARRAY
I	Node number
X(I,1)	X - coordinate
X(I,2)	Y - coordinate
	ELEMENT ARRAY
I	Element number

NOD(I,J)	Nodal point number(J=1,2,3,4)
THICK(I)	Thickness of an element
NEP(I)	Element elastic property number

BOUNDARY ARRAY

NF(I)	Nodal point number with prescribed displacement
NB(I,1) .	Boundary node index relative to X - direction (= 0 for no translation; = 1 for translation allowed
NB(I,2)	Boundary node index relative toY - direction (= 0 for no translation; = 1 for translation allowed
BV(I,1)	Magnitude of prescribed translation in X - direction
BV(I,2)	Magnitude of prescribed translation in Y - direction

PARTITION ARRAY

NSTART(I)	Number of the first element in the partition
NEND(I)	Number of the last element in a partition
NFIRST(I)	Number of the first nodal point in a

	partition
NLAST(I)	Number of the last nodal point in a partition

ELASTIC PROPERTIES

E1(I)	Modulus of elasticity in X - direction
E2(I)	Modulus of elasticity in Y - direction
P1(I)	Poisson's ratio in X - direction
P2(I)	Poisson's ratio in Y - direction

INITIAL LOAD ARRAY

K	Loaded nodal point number
U(2k-1,1)	Initial load in X - direction
U(2k,1)	Initial load in Y - direction

LOADING SEQUENCE

NELEMS	Number of spring elements
NSTEPS	Number of loading steps
DELTAX	Load increment in X - direction
DELTAY	Load increment in Y - direction
BTH	Width of the analysed member

SPRING ELEMENT ARRAY

I	Spring number
NODS(I,1)	Concrete node connected to spring

NODS(I,2)	Steel node connected to spring
NSSS(I)	Spring position indicator 1= internal, 0= external
WDT(I)	Effective spring length
BN(I)	Angle of inclination of stirrup to global X - axis
DIA(I)	Average diameter of bars connected to the spring
ENUM(I)	Number of bars connected to the spring

SPRING ELEMENT COUNTER ARRAY

NCHK(I)	Number of spring elements in partition I
NSPGST(I)	Number of first spring element in partition I
NSPGED(I)	Number of last spring element in partition I

STIRRUP COUNTER ARRAY

NSTR(I)	Number of stirrups in partition I
NENDST(I,1)	Number of first stirrup in partition I
NENDST(I,2)	Number of last stirrup in partition I

STIRRUP ARRAY

I	Stirrup number
NODSTR(I,J)	First and second node number(J=1,2)

STR(I,1)	Area of stirrup

CONCRETE PARAMETERS

FO	Maximum concrete stress
FF	Concrete stress at maximum strain
SEF	Maximum concrete strain
RUPTR	Modulus of rupture uf concrete

STEEL PARAMETERS

EY	Yield strain of steel
ESTRH	Strain at onset of strain hardening
ESH	Initial strain hardening modulus
PSH	Poisson's ratio in strain hardening zone

DATAS FOR TEST BEAM 1

STRUCTURE PROPERTIES

3 120 88 11 1 2 1 2 0

NODAL POINT ARRAY

1	0.0	0.0
2	0.0	1.07536
3	0.0	1.07536
4	0.0	2.04965
5	0.0	2.04965
6	0.0	4.0

7	0.0	8.0
8	0.0	12.0
9	0.0	16.0
10	0.0	20.0
11	2.0	0.0
12	2.0	1.07536
13	2.0	1.07536
14	2.0	2.04965
15	2.0	2.04965
16	2.0	4.0
17	2.0	8.0
18	2.0	12.0
19	2.0	16.0
20	2.0	20.0
21	8.0	0.0
22	8.0	1.07536
23	8.0	1.07536
24	8.0	2.04965
25	8.0	2.04965
26	8.0	4.0
27	8.0	8.0
28	8.0	12.0
29	8.0	16.0
30	8.0	20.0
31	14.0	0.0

32	14.0	1.07536
33	14.0	1.07536
34	14.0	2.04965
35	14.0	2.04965
36	14.0	4.0
37	14.0	8.0
38	14.0	12.0
39	14.0	16.0
40	14.0	20.0
41	20.0	0.0
42	20.0	1.07536
43	20.0	1.07536
44	20.0	2.04965
45	20.0	2.04965
46	20.0	4.0
47	20.0	8.0
48	20.0	12.0
49	20.0	16.0
50	20.0	20.0
51	26.0	0.0
52	26.0	1.07536
53	26.0	1.07536
54	26.0	2.04965
55	26.0	2.04965
56	26.0	4.0

57	26.0	8.0
58	26.0	12.0
59	26.0	16.0
60	26.0	20.0
61	32.0	0.0
62	32.0	1.07536
63	32.0	1.07536
64	32.0	2.04965
65	32.0	2.04965
66	32.0	4.0
67	32.0	8.0
68	32.0	12.0
69	32.0	16.0
70	32.0	20.0
71	38.0	0.0
72	38.0	1.07536
73	38.0	1.07536
74	38.0	2.04965
75	38.0	2.04965
76	38.0	4.0
77	38.0	8.0
78	38.0	12.0
79	38.0	16.0
80	38.0	20.0
81	44.0	0.0

82	44.0	1.07536
83	44.0	1.07536
84	44.0	2.04965
85	44.0	2.04965
86	44.0	4.0
87	44.0	8.0
88	44.0	12.0
89	44.0	16.0
90	44.0	20.0
91	51.0	0.0
92	51.0	1.07536
93	51.0	1.07536
94	51.0	2.04965
95	51.0	2.04965
96	51.0	4.0
97	51.0	8.0
98	51.0	12.0
99	51.0	16.0
100	51.0	20.0
101	58.0	0.0
102	58.0	1.07536
103	58.0	1.07536
104	58.0	2.04965
105	58.0	2.04965
106	58.0	4.0

107	58.0	8.0
108	58.0	12.0
109	58.0	16.0
110	58.0	20.0
111	65.0	0.0
112	65.0	1.07536
113	65.0	1.07536
114	65.0	2.04965
115	65.0	2.04965
116	65.0	4.0
117	65.0	8.0
118	65.0	12.0
119	65.0	16.0
120	65.0	20.0

ELEMENT ARRAY

1	11	12	2	1.0	1
2	12	14	4	0.82996	1
3	13	15	5	0.17004	2
4	14	16	6	1.0	1
6	16	17	7	1.0	1
7	17	18	8	1.0	1
8	18	19	9	1.0	1
9	19	20	10	1.0	1
11	21	22	12	1.0	1

12	22	24	14	0.82996	1
13	23	25	15	0.17004	2
14	24	26	16	1.0	1
16	26	27	17	1.0	1
17	27	28	18	1.0	1
18	28	29	19	1.0	1
19	29	30	20	1.0	1
21	31	32	22	1.0	1
22	32	34	24	0.82996	1
23	33	35	25	0.17004	2
24	34	36	26	1.0	1
26	36	37	27	1.0	1
27	37	38	28	1.0	1
28	38	39	29	1.0	1
29	39	40	30	1.0	1
31	41	42	32	1.0	1
32	42	44	34	0.82996	1
33	43	45	35	0.17004	2
34	44	46	36	1.0	1
36	46	47	37	1.0	1
37	47	48	38	1.0	1
38	48	49	39	1.0	1
39	49	50	40	1.0	1
41	51	52	42	1.0	1
42	52	54	44	0.82996	1

43	53	55	45	0.17004	2
44	54	56	46	1.0	1
46	56	57	47	1.0	1
47	57	58	48	1.0	1
48	58	59	49	1.0	1
49	59	60	50	1.0	1
51	61	62	52	1.0	1
52	62	64	54	0.82996	1
53	63	65	55	0.17004	2
54	64	66	56	1.0	1
56	66	67	57	1.0	1
57	67	68	58	1.0	1
58	68	69	59	1.0	1
59	69	70	60	1.0	1
61	71	72	62	1.0	1
62	72	74	64	0.82996	1
63	73	75	65	0.17004	2
64	74	76	66	1.0	1
66	76	77	67	1.0	1
67	77	78	68	1.0	1
68	78	79	69	1.0	1
69	79	80	70	1.0	1
71	81	82	72	1.0	1
72	82	84	74	0.82996	1
73	83	85	75	0.17004	2

74	84	86	76	1.0	1
76	86	87	77	1.0	1
77	87	88	78	1.0	1
78	88	89	79	1.0	1
79	89	90	80	1.0	1
81	91	92	82	1.0	1
82	92	94	84	0.82996	1
83	93	95	85	0.17004	2
84	94	96	86	1.0	1
86	96	97	87	1.0	1
87	97	98	88	1.0	1
88	98	99	89	1.0	1
89	99	100	90	1.0	1
91	101	102	92	1.0	1
92	102	104	94	0.82996	1
93	103	105	95	0.17004	2
94	104	106	96	1.0	1
96	106	107	97	1.0	1
97	107	108	98	1.0	1
98	108	109	99	1.0	1
99	109	110	100	1.0	1
101	111	112	102	1.0	1
102	112	114	104	0.82996	1
103	113	115	105	0.17004	2
104	114	116	106	1.0	1

106 116 117 107 1.0 1

107 117 118 108 1.0 1

108 118 119 109 1.0 1

109 119 120 110 1.0 1

BOUNDARY ARRAY

11 1 0 0.0

111 0 1 0.0

112 0 1 0.0

113 0 1 0.0

114 0 1 0.0

115 0 1 0.0

116 0 1 0.0

117 0 1 0.0

118 0 1 0.0

119 0 1 0.0

120 0 1 0.0

PARTITION ARRAY

1 32 1 40

25 64 41 80

57 88 81 120

ELASTIC PROPERTIES

3834253.0 3834253.0 0.2 0.2

29000000.0 29000000.0 0.3 0.3

INITIAL LOAD ARRAY

90	0.0	-1120.0	

LOADING SEQUENCE

24	20	0.0	-100.0	12.0	

SPRING ELEMENT ARRAY

2	3	0	1.0	0.0	1.125	2.0
4	5	1	1.0	0.0	1.125	2.0
12	13	0	4.0	0.0	1.125	2.0
14	15	1	4.0	0.0	1.125	2.0
22	23	0	6.0	0.0	1.125	2.0
24	25	1	6.0	0.0	1.125	2.0
32	33	0	6.0	0.0	1.125	2.0
34	35	1	6.0	0.0	1.125	2.0
42	43	0	6.0	0.0	1.125	2.0
44	45	1	6.0	0.0	1.125	2.0
52	53	0	6.0	0.0	1.125	2.0
54	55	1	6.0	0.0	1.125	2.0
62	63	0	6.0	0.0	1.125	2.0
64	65	1	6.0	0.0	1.125	2.0
72	73	0	6.0	0.0	1.125	2.0
74	75	1	6.0	0.0	1.125	2.0
82	83	0	6.5	0.0	1.125	2.0
84	85	1	6.5	0.0	1.125	2.0

92	93	0	7.0	0.0	1.125	2.0
94	95	1	7.0	0.0	1.125	2.0
102	103	0	7.0	0.0	1.125	2.0
104	105	1	7.0	0.0	1.125	2.0
112	113	0	3.5	0.0	1.125	2.0
114	115	1	3.5	0.0	1.125	2.0

SPRING ELEMENT COUNTER ARRAY

8

1 8

8

9 16

8

17 24

STIRRUP COUNTER ARRAY

0

0

0

0

CONCRETE PARAMETERS

4000.0	3700.0	0.003	650.0

STEEL PARAMETERS

0.00132	0.018	500000.0	0.5